

Mutation Invariants of Alternating Virtual Knots

Damian Lin

An essay submitted in partial fulfilment of
the requirements for the degree of
Bachelor of Science/Bachelor of Advanced Studies (Honours)

Pure Mathematics
University of Sydney



May 24, 2023

Contents

Introduction	3
Acknowledgements	5
1 Knots and the Lattice of Integer Flows	6
1.1 Knots and Knot Invariants	6
1.2 Connected Sums and Prime Knots	8
1.3 Alternating Knots, Knot Mutation and the Tait Graph	9
1.4 The Lattice of Integer Flows	13
1.5 Heegaard-Floer Homology and the d -invariant	19
2 Virtual Knots	21
2.1 Knots in Thickened Surfaces	21
2.2 Stable Equivalence and Virtual Knots	23
2.3 Diagrams with Virtual Crossings	24
2.4 Annular Connected Sums and Prime Virtual Knots	26
2.5 Alternating Virtual Knots and Virtual Knot Mutation	27
2.6 Checkerboard Colourings and Tait Graphs of Virtual Knots	28
2.7 The Lattice of Integer Flows for Virtual Knots	30
3 Gordon-Litherland Linking Forms	34
3.1 Spanning Surfaces and Linking Numbers	34
3.2 The Linking Form	35
3.3 The Gordon-Litherland Pairing	37
4 Computing Mock Seifert Matrices	39
4.1 Gauss Codes and Gauss Diagrams	39
4.2 Reconstructing the Ribbon Tait Graph	41
4.3 Mock Seifert Matrices: Preliminaries	45
4.4 Computing Mock Seifert Matrices	48
4.5 Incompleteness of the Virtual Gordon-Litherland Pairing	50
4.6 A Note on Invariants of Unimodular Congruence	52
A Python Implementation of Algorithms	58

Introduction

Since the very beginnings of knot theory, a particular class of knots - alternating knots - have stood out. An alternating knot is a knot that can be presented in a diagram in which crossings alternate over and under as the knot is traversed. Such a diagram is called an alternating diagram for the knot. Alternating knots were the subject of three famous conjectures made by P.G. Tait in the 19th century in his attempt to tabulate knots. The first Tait conjecture states that any reduced alternating knot diagram has the fewest possible crossings across all diagrams of that knot. Tait's second conjecture asserts that knots which are their own mirror images have an even number of positive and negative crossings. Finally, Tait conjectured that all alternating diagrams of a knot are related by a sequence of certain moves known as flypes.

Much to Tait's credit, all three of these conjectures - and even more of his conjectures about alternating knots - turned out to be true! With the advent of the Jones polynomial, the first two were proven in 1987 by Kauffman [Kau87], Murasugi [Mur87] and Thistlethwaite [Thi87], each working independently. The final conjecture would remain unsolved until 1991 when it was proved by Thistlethwaite and Menasco [MT93].

Despite this progress, a geometric characterisation of alternating knots (one not based purely on knot diagrams) remained elusive, prompting the quote '*What is an alternating knot?*' from Ralph Fox. This question was answered by Greene in 2017 [Gre17], who resolves that alternating knots are precisely those knots that bound both positive definite and negative definite spanning surfaces with respect to the Gordon-Litherland pairing, with a similar result by Howie at the same time [How17]. Greene then uses this characterisation, combined with the *discrete Torelli theorem* - a graphical analogue of a result in algebraic geometry - to give the first geometric proofs of some of Tait's conjectures.

The relationship between knots and graphs is a classical construction of Tait's, known as the Tait graph. In a separate breakthrough result [Gre11], Green manifests this correspondence to completely characterise alternating knots up to *Conway mutation*. He uses the discrete Torelli theorem to show that a lattice-theoretic construction - the d -invariant of the Tait graph - completely captures the information of the alternating knot, modulo mutation. Greene also proves that this lattice-theoretic d -invariant coincides with a topological construction: the d -invariant of the Heegaard-Floer homology of the double branched-cover of the knot.

This essay is devoted to an analogue of this story in a more general setting: that of knots in thickened surfaces, also known as virtual knots. Virtual knots are the subject of a rich, modern branch of knot theory. They have several definitions of independent interest: combinatorial [Kau99; GPV00], geometric [Kup03; CKS00], algebraic [BD16; BD17]

and computational [Kau99]. In recent work Boden-Chrisman-Karimi have extended the Gordon-Litherland pairing to virtual knots [BCK22].

By equating Greene's d -invariant with the virtual Gordon-Litherland pairing, we find that the d -invariant does generalise to a mutation invariant of alternating virtual knots. By constructing a counterexample using computational methods, we will show that this generalisation is not a complete invariant up to mutation.

In Chapter 1, we review the necessary notions of classical knot theory, and associate a pair of lattices to each knot, equivalent to Green's d -invariant construction. In Chapter 2, we introduce knots in thickened surfaces, allowing for a geometric definition of virtual knots as equivalence classes of these. We then follow a similar path as in Chapter 1, observing that Greene's d -invariant does extend to the virtual setting, but finding that the classical proof of its completeness breaks down. In Chapter 3, we examine the Gordon-Litherland linking form, another mutation invariant of alternating classical knots, and review its extension to the virtual setting by Boden-Chrisman-Karimi. In Chapter 4, we describe computer algorithms to compute the Gordon-Litherland linking form from tables of virtual knots, and present a counterexample to the completeness of the virtual d -invariant, found using these algorithms.

I have contributed significantly to the theoretical results presented in this essay, along with Hans Boden and Zsuzsanna Dancso. The algorithm given in Section 4.2 is joint work with Tilda Wilkinson-Finch. The later computational results in this text are my sole work.

I plan to submit two journal publications based on the results of this thesis: one - mostly theoretical - joint with Boden, Dancso, and Wilkinson-Finch, which is currently in draft form; and one - mostly computational - as a sole author.

Acknowledgements

Firstly, I would like to express my gratitude to my supervisor, Zsuzsanna Dancso, for all of the time, effort and faith she has poured into me over the last year. Thank you, Zsuzsi for your encouragement to persevere at times when I was stuck, your sage advice on things mathematical and practical, and your ability to give everything a personal touch. I do not think I could have chosen a better supervisor for my honours year.

I am also very thankful to my collaborators: Hans Boden and Tilda Wilkinson-Finch, for many delightful and insightful conversations. Thanks especially to Hans for his mathematical encouragement and guidance, in particular, insights into several proofs.

My thanks also goes to the knot at lunch group for creating a cosy environment and making me look forward to the ritual of Monday lunch.

Finally I would like to thank my family and friends for their support, their encouragement, and their love.

Chapter 1

Knots and the Lattice of Integer Flows

*"A knot!" said Alice, "oh, do let me help to undo it!"
"I shall do nothing of the sort!" said the mouse.*

— Lewis Carroll, *Alice's Adventures in Wonderland*

1.1 Knots and Knot Invariants

We begin with a swift introduction to the rich and marvellous study of tangled-up pieces of string: the theory of knots. Despite being a complex and intricate field, any child can intuitively grasp the concept of a knot as a closed loop of string in space. To formalise this and remove any pathological examples that are inconsistent with this intuition, we define a *knot* to be an injective embedding of the circle into 3-space, $K : \mathbb{S}^1 \hookrightarrow \mathbb{R}^3$. The requirement that the embedding be injective ensures that the string does not intersect itself. Fig. 1 gives a few example knots.

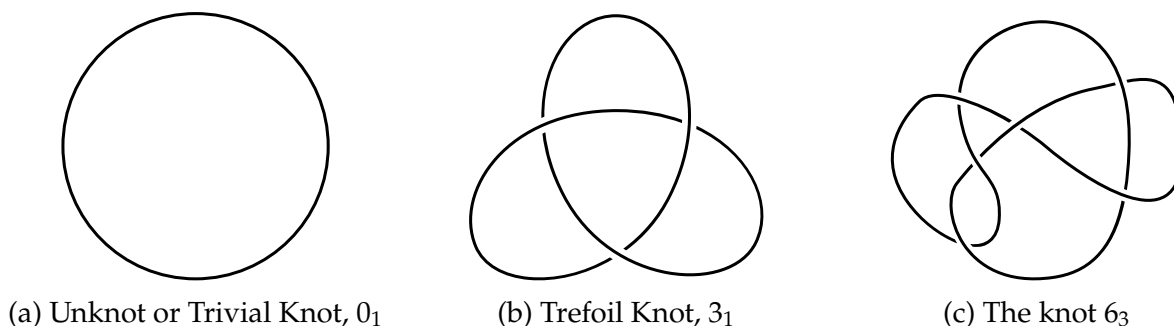


Figure 1: Some examples of knots, presented through knot diagrams. Their names in the Rolfsen knot table are also given.

The example in Fig. 2a shows a knot that can be ‘untwisted’ to look like the example in Fig. 1a. In general, we do not distinguish between knots if there is some way to deform one, without breaking the circle or passing it through itself, into the other. We say two knots K_1 and K_2 are *equivalent* or equal if there is an *ambient isotopy* from K_1 to K_2 ; that is, a continuous map

$$F : \mathbb{R}^3 \times I \longrightarrow \mathbb{R}^3$$

such that at each $t \in I$, the corresponding $f_t : \mathbb{R}^3 \rightarrow \mathbb{R}^3$ is a homeomorphism of \mathbb{R}^3 , and f_0 is the identity map on \mathbb{R}^3 , while $f_1 \circ K_1 = K_2$.

Though a central objective of knot theory is to classify knots up to ambient isotopy, it can be hard to write down explicit ambient isotopies directly. Rather, we use other means to classify knots which will be the subject of the remainder of this section.

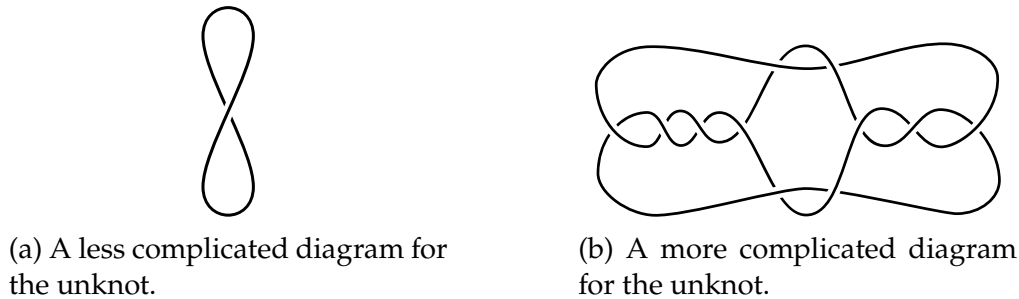


Figure 2: It can be difficult to tell whether two diagrams represent the same knot. The diagram in (b) is from [Goe34].

Though we claimed that the objects in Fig. 1 were knots, they are really projections of knots onto the plane with markings we call *crossings* to make clear that some *strand* of the knot passes over another strand. We refer to these objects as *knot diagrams*. We consider diagrams equivalent up to planar isotopy as 4-valent graphs. In other words, diagrams can just as well be thought of as combinatorial objects consisting of a list of crossings with labelled ends, and a description of how these ends connect. So long as the ends are connected in a planar way, the exact path that connects them is unimportant.

Different diagrams can represent the same knot: for example, the diagrams in Fig. 1a and Fig. 2a, as the latter could be ‘untwisted’ into the former. It is not always obvious when two diagrams represent the same knot. An example is Fig. 2b, yet another diagram for the unknot, but it may not be immediately obvious how this knot can be untangled. The unknot is not special here – every knot has many diagrams, and there is no upper bound on the number of crossings, as we could continually add twists to an arc to create diagrams with arbitrarily many crossings for any knot. However, each knot does have a lower bound on the number of crossings any diagram representing it can have, which we call its *crossing number*. For example, the crossing number of the unknot is 0, and the crossing number of the Trefoil knot is 3, and this lower bound is realised in the diagram in Fig. 1b.

Diagrams are easier to work with than embeddings, thanks to the following foundational theorem due to Alexander-Briggs [AB26] and independently Kurt Reidemeister [Rei27].

Theorem. (*The Reidemeister Theorem*) *Two knot diagrams D_1 and D_2 represent equivalent knots if and only if there is some sequence of finitely many moves of the types given in Fig. 3 that transform D_1 into D_2 .*

The early study of knot theory by pioneers such as P.G. Tait, C.N. Little and T. Kirkman involved trying to find, by hand, sequences of moves to show two knots were equivalent.

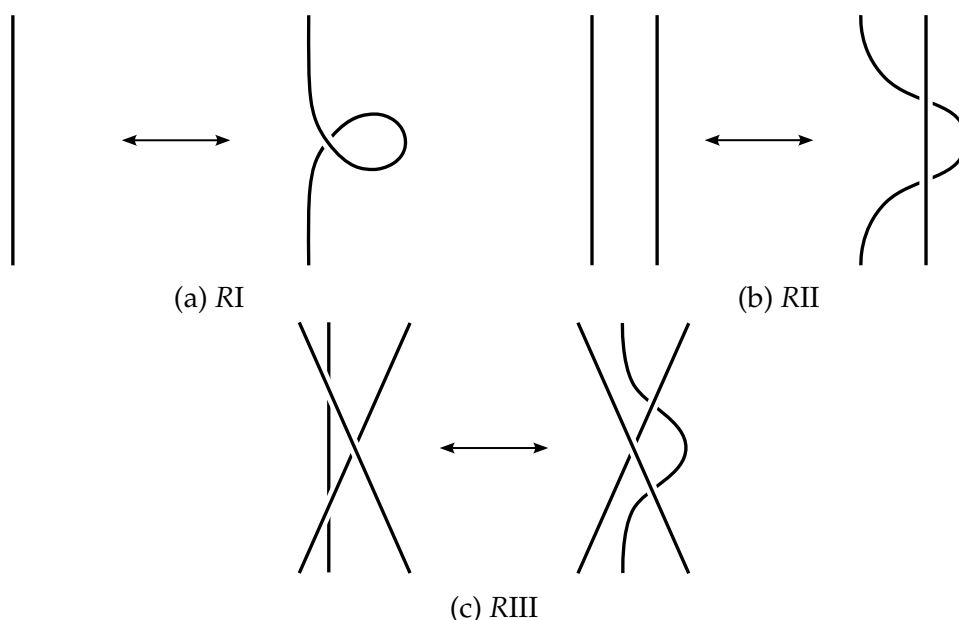


Figure 3: The Reidemeister moves.

And in hindsight they did remarkably well with so few tools. But Tait himself noted that it was impossible by these means alone to ever prove that two knots were distinct. The modern way we do this is by using knot invariants. If we define some map from knot diagrams to some other class of objects, perhaps a truth value, a polynomial, or a group, and show that none of the Reidemeister moves changes the value of this map, then we have a well-defined function on knots: a *knot invariant*. This allows us to prove that two knots are different, for if they take on different values under some invariant, they must be distinct.

However, invariants are one-sided in nature. Taking different values can tell us that two knots are different, but two knots taking on the same value of some invariant doesn't necessitate that they be equivalent knots. Such an invariant – one that is an injective function from the class of knots – is called a *complete invariant*, and while we now know of a zoo of different invariants, we have yet to find what is perhaps the Holy Grail of knot theory: a complete invariant that is also easy to compute.

1.2 Connected Sums and Prime Knots

In order to classify knots, it is helpful to be able to build large knots out of smaller ones, and vice-versa, decompose complicated knots into their simpler “atomic” pieces.

Given knots K_1 and K_2 , we define the connected sum, $K_1 \# K_2$ as illustrated in Fig. 4. Take K_1 and K_2 and remove a small arc from each knot, then reconnect the two cut knots to form $K_1 \# K_2$.

If K_1 and K_2 are oriented (equipped with a direction) then there is only one way to connect the cut ends in an orientation-preserving way. Otherwise there are two choices. This choice aside, $K_1 \# K_2$ is well-defined, as regardless which arc of K_1 we attached K_2 to,

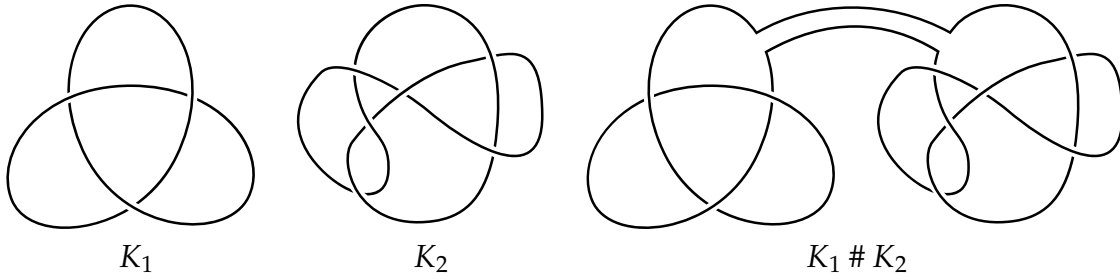


Figure 4: Example of a connected sum with $K_1 = 3_1$ and $K_2 = 6_3$.

we could shrink K_2 to an arbitrarily small size, then pull it around K_1 to any desired spot, then re-enlarge it. Likewise, the arc chosen on K_2 does not matter, so the connect sum is independent of choice of arc. In fact, this operation is also associative and commutative [BZH13, Corollary 7.13].

There is a corresponding definition of connected sum for knot diagrams, where the arcs to cut are chosen on the periphery of each diagram and connected in a planar way (without introducing additional crossings).

With this, we have a way of expressing more complicated knots in terms of less complicated knots. We call a knot *prime* if there is no way to write it as the connected sum of non-trivial knots. The only exception is the unknot, which we define not to be prime. Similarly, we call a knot *composite* if there is a way to write it as the connected sum of at least two knots, none of which is the trivial knot. In this way, the prime knots and the connected sum are in analogy with the prime numbers and multiplication. There is even a unique decomposition theorem for knots, just as for prime numbers [BZH13, Theorem 7.12]:

Theorem (Schubert's Theorem). *Each non-trivial knot K is a finite connected sum of prime knots and these factors are uniquely determined, up to permutation.*

1.3 Alternating Knots, Knot Mutation and the Tait Graph

Alternating knots are of particular interest in knot theory, and they possess a number of interesting properties. We call a knot diagram *alternating* if, traversing the diagram, the crossings alternate under and over. For every diagram that is alternating, it is possible to construct a non-alternating diagram of an equivalent knot: one simply needs to apply a type RI Reidemeister move appropriately to any strand of the knot: for example the alternating diagram of the Trefoil knot in Fig. 1b transforms into the non-alternating diagram in Fig. 5a. Hence we define an *alternating knot* as a knot which can be represented by an alternating diagram. For low crossing-number, that is for knots that can be represented by diagrams with few crossings, many of the knots are alternating, but this trend quickly reverses as crossing number is increased.

Alternating knots also have a purely geometrical characterisation, based on the knot itself rather than its diagrams. The result by Greene [Gre17] asserts that alternating knots are exactly those knots that simultaneously bound positive definite and negative definite

surfaces with respect to the Gordon-Litherland linking form. This will be examined in Chapter 3.

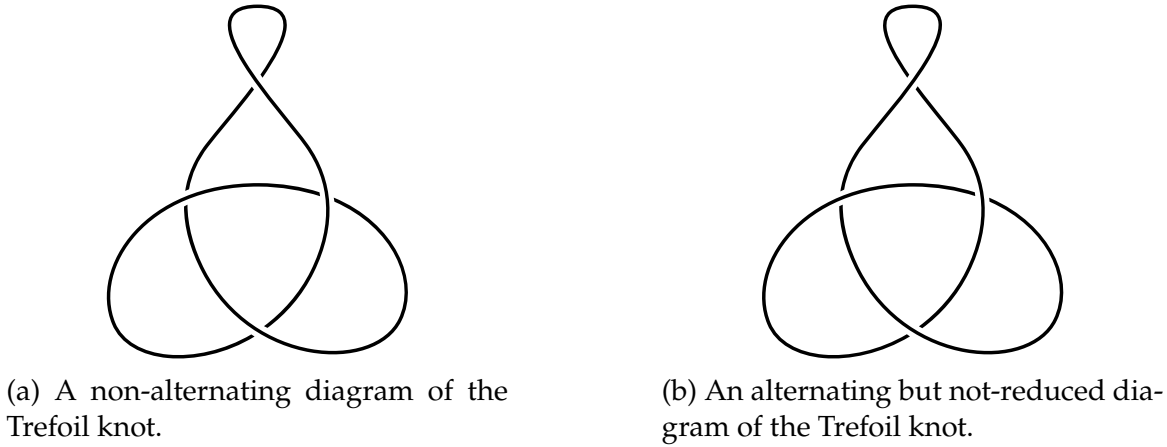


Figure 5: Diagrams of the Trefoil knot.

Tait made a series of conjectures about alternating knots in his early attempts to tabulate knots. The first conjecture is about the crossing number of alternating knots and was proven in 1987 by Kaufmann, Murasugi and Thistlethwaite, all independently [Kau87; Mur87; Thi87]. Nonetheless it remains known as the first Tait conjecture.

An alternating knot diagram is *reduced* if there are no nugatory crossings. A *nugatory crossing* is a crossing for which there is a circle in the projection plane of the knot diagram which intersects the diagram transversely at that crossing, but nowhere else. Nugatory crossings are those which could be immediately undone to simplify the knot diagram. The diagram in Fig. 1b is a reduced alternating diagram, while the diagram in Fig. 5b is alternating but not reduced.

Theorem (First Tait Conjecture). *Let D be a reduced alternating knot diagram for a knot K . Then D has minimal crossing number.*

The third of these conjectures is known as the flyping conjecture, and it relates reduced alternating diagrams of the same alternating knot by moves known as flype moves.

A *tangle* in a knot diagram is a region of the plane that is homeomorphic to a disc, such that the knot crosses the boundary of the disc exactly four times, as in Fig. 9a and Fig. 9b. A *flype* move is a diagrammatic move that flips a tangle but does not alter the knot type, as in Fig. 6.

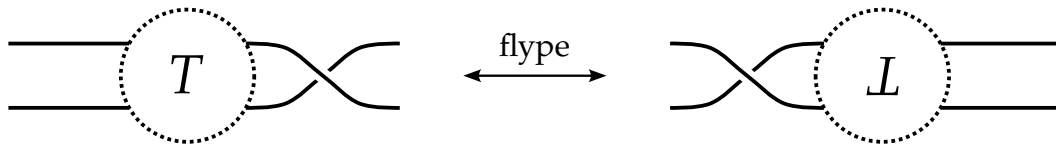


Figure 6: A general flype move.

Flype moves preserve whether diagrams alternate:

Proposition. *Let D be an alternating diagram. Then any flype of D is an alternating diagram.*

Proof. Assume that D is an alternating diagram. There are three cases for the connectivity of the tangle T in D , given in Fig. 7.

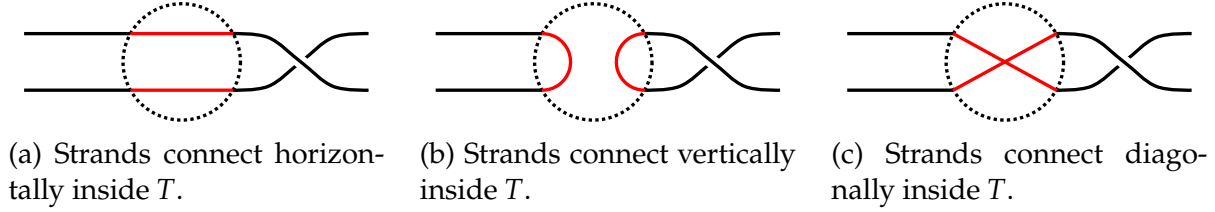


Figure 7: Three cases for the connectivity inside a tangle.

In the first case, the strands connect horizontally. Consider the strand that enters the tangle at the top right. In the tangle it intersects itself some number of times before exiting the tangle at the top left. Since it goes over and under itself once at each self-crossing, this contributes an even number of encounters. By the Jordan curve theorem, it also encounters the bottom strand an even number of times. So both strands have an even number of crossing encounters along them.

We must prove the alternating property is preserved by the flype at the boundaries of the tangle. The flype affects the diagram in two ways. Firstly, it performs a horizontal flip on the tangle. This swaps the two strands inside the tangle, but also sends over-crossings to under-crossings. Hence in this case, whether there is an over- or under-strand just inside the boundary of T is unaffected. Secondly, it moves the crossing outside the tangle to the other side. The illustration in Fig. 8 shows that these two effects preserve the alternating property at the boundaries of T . This proves the case in Fig. 7a, and the cases in Fig. 7b and Fig. 7c are similar. \square

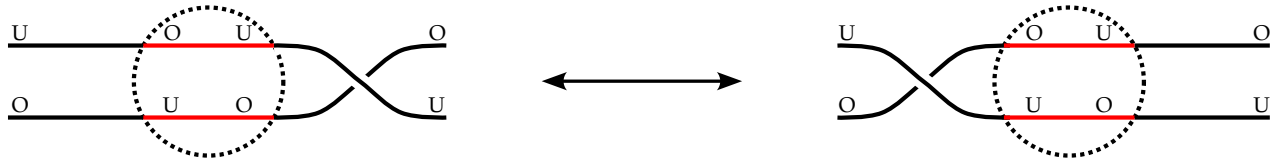


Figure 8: Flypes preserve the alternating property.

The flying theorem was proven by Menasco and Thistlethwaite in [MT93, p. 166]:

Theorem (Flying Theorem). *Any two reduced alternating diagrams, D and E of the same prime knot, are related by a sequence of flypes.*

This is a Reidemeister-like theorem for alternating knots in that it relates equivalence of diagrams to the existence of a sequence of moves between them, only going via alternating diagrams, and without increasing crossing number.

Knot mutation is another way of constructing new knots from existing ones, preserving the alternating property. If we take a diagram, choose a tangle, and then perform a

reflection (up to planar isotopy) of that tangle, either reflecting it left-right or up-down, or across one of the diagonals, the corresponding operation on the knot is known as *mutation*, and the two knots are called *mutants*. Mutants are some of the hardest knots to distinguish, as many of their invariants are the same. An example of this is the Conway the Kinoshita-Terasaka knots, given in Fig. 9.

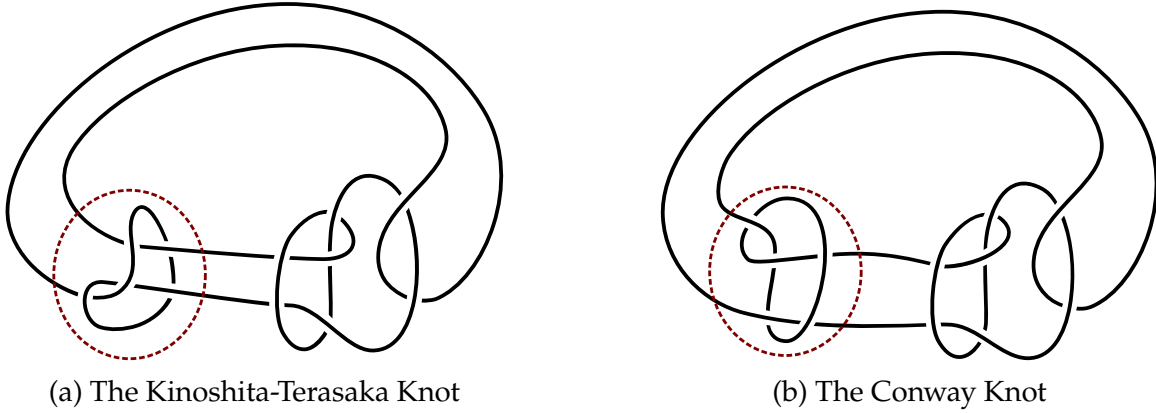


Figure 9: The Kinoshita-Terasaka mutants. These are the two non-trivial knots of lowest crossing number that have trivial Alexander polynomial. The disk of mutation is marked. The projections used for these diagrams were taken from [Ada94, Fig. 2.32].

To a knot diagram, we associate two graphs known as the *Tait graphs*, shown in Fig. 10 and explained as follows. We interpret the knot diagram as a tetravalent planar graph that divides the plane into regions. By an application of the Jordan curve theorem, it is possible to colour these regions two colours, black and white, such that adjacent regions are never the same colour. Such a colouring is called a *checkerboard colouring*. Note that in a checkerboard colouring, regions that are diagonal to each other at crossings are necessarily the same colour.

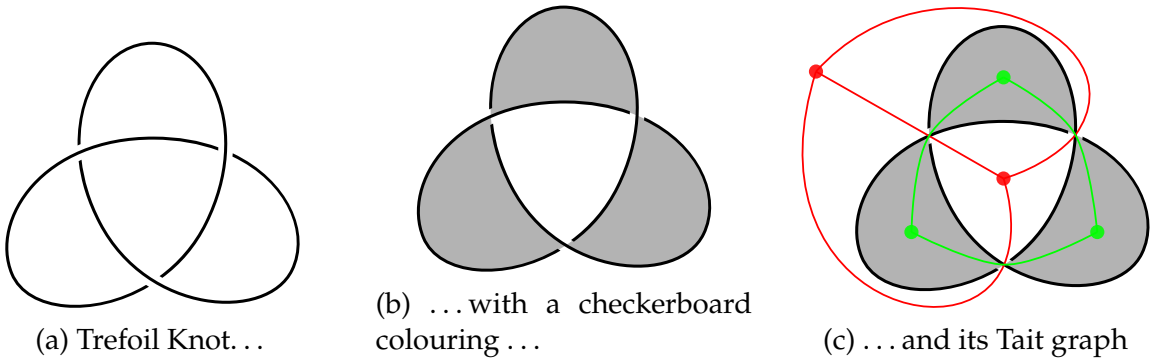


Figure 10: Producing the Tait graph(s) of the trefoil knot.

In the checkerboard colouring of a diagram, the colouring around each crossing can look one of two ways. According to this, we call the crossings either Type A or Type B. In an alternating diagram, all crossings will have the same type [Thi87, p. 300]. The convention

for alternating knots is to choose the checkerboard colouring such that all crossings are type A.



Figure 11: Crossing Type

A checkerboard colouring of a knot diagram specifies two not-necessarily orientable spanning surfaces for the knot: a spanning surface is a surface embedded in \mathbb{R}^3 whose boundary is the knot. These spanning surfaces are obtained by attaching disks for each coloured region by twisted bands for each crossing, where the twisting direction is specified by the type of the crossing. The convention that all crossings be of type A corresponds with the convention that the black surface be positive definite with respect to the linking form on its first homology. This will be explained further in Chapter 3.

To construct the black Tait graph $G_B(D)$, we place a vertex in every black region of the plane. For each crossing we draw an edge between the vertices corresponding to the black region on either side of the crossing, obtaining a planar graph, potentially with multiple edges. The white Tait graph $G_W(D)$ is constructed similarly from the vertices corresponding to white regions.

Either of these graphs, along with their plane embeddings, retain enough information to construct the other. The *planar dual* of G, G^* , is the graph obtained by replacing every face in the plane embedding of G with a vertex, and every edge in G that separates two faces becoming an edge between the corresponding vertices in G^* . It can be easily seen from the way Tait graphs are constructed in Fig. 10 that the two Tait graphs are planar duals: $G_B(D)^* = G_W(D)$ and $G_W(D)^* = G_B(D)$. Because both planar graphs can be constructed from each other, we sometimes refer to either one as *the* Tait graph of a knot. Later we will examine the more general class of knots in thickened surfaces, for which this duality breaks down, and we will need both Tait graphs.

If we have the Tait graph of an alternating diagram of a knot, we can reconstruct the knot diagram by placing a crossing on every edge of the Tait graph, as seen in Fig. 12a. Connecting up the crossings by strands along the Tait graph, as in Fig. 12b, reconstructs the knot diagram, up to planar isotopy.

1.4 The Lattice of Integer Flows

For the rest of this chapter, we introduce the lattice of integer flows of a graph, then largely following [Gre11], we show that the lattice of integer flows of the Tait graph is a complete mutation invariant of alternating knots. This means that it is both an invariant

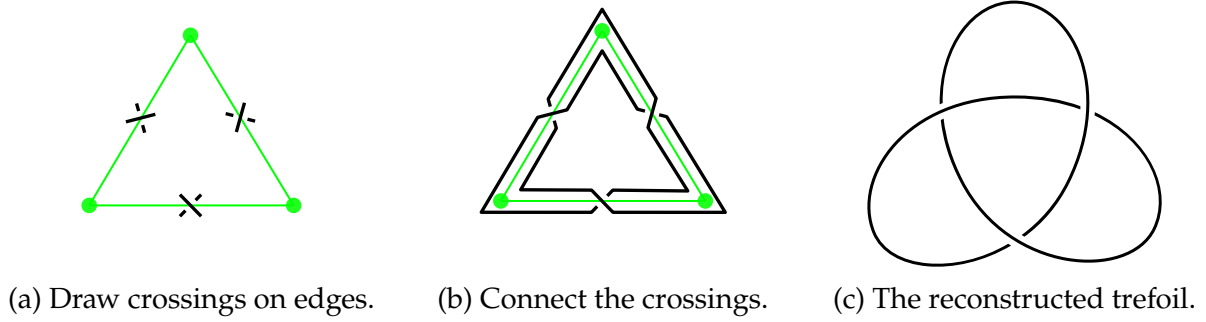


Figure 12: Reconstructing a knot diagram from its Tait graph.

of alternating knots, and takes the same value on alternating knots if and only if they are mutants. We then talk about the equivalent formulation given in [Gre11] as the d -invariant.

A *lattice* is a finitely generated free abelian group L , equipped with an inner product $\langle \cdot, \cdot \rangle : L \times L \rightarrow \mathbb{R}$. All lattices in this text will be *integral lattices*, meaning the inner product's image is contained within \mathbb{Z} . An *isomorphism of lattices* is a bijection $\psi : L_1 \rightarrow L_2$ that preserves the inner product, that is, $\langle x, y \rangle_1 = \langle \psi(x), \psi(y) \rangle_2$ for all $x, y \in L_1$.

Let $G = (E, V)$ be a finite, connected graph (in which loops and multiple edges are allowed) with vertex set V and edge set E . In particular, G is a 1-dimensional CW-complex with boundary map $\partial : C_1(G) \rightarrow C_0(G)$. In the edge basis of $C_1(G)$ and vertex basis of $C_0(G)$, this is a map $\mathbb{Z}^E \rightarrow \mathbb{Z}^V$, and is represented by the $|V| \times |E|$ incidence matrix D with entries given by

$$D_{ij} = \begin{cases} +1 & \text{if } e_i \text{ is oriented into } v_j, \\ -1 & \text{if } e_i \text{ is oriented out of } v_j, \\ 0 & \text{if } e_i \text{ is a loop at } v_j \text{ or is not incident to } v_j. \end{cases}$$

The *lattice of integer flows* of G is the free abelian group $\Lambda(G) = \ker \partial$, along with the inner product induced by the Euclidean inner product on \mathbb{Z}^E . Equivalently, $\Lambda(G)$ is the first homology group of G , with inner products taken in $C_1(G)$. While the lattice $\Lambda(G)$ may depend on the orientation of the edges in G , its isomorphism class does not, as the isomorphism class of the homology group is independent of orientation, and the Euclidean inner product is preserved by sending an edge to its negation: $\langle e_i, e_i \rangle = \langle -e_i, -e_i \rangle = 1$, and $\langle e_i, e_j \rangle = \langle -e_i, e_j \rangle = 0$ for $i \neq j$.

As an example, let D be the diagram of the Trefoil knot given in Fig. 10. The Tait graphs of the trefoil knot are shown in Fig. 13. We compute the lattice of integer flows of each of these graphs, $\Lambda(G_B(D))$ and $\Lambda(G_W(D))$. Rather than use this cumbersome notation, we shorten this to $\Lambda_W(D)$ or $\Lambda_B(D)$ for the lattice of integer flows of the Tait graph corresponding to the white/black regions, respectively. We orient the graphs arbitrarily to compute the lattice of integer flows, but as we will see the invariant produced is independent of this choice. We start with the more typical lattice of integer flows: that of the Tait graph corresponding to the white region (red in Fig. 13). There are two independent cycles, $-f_1 + f_2$ and $-f_2 + f_3$, so $\Lambda_B(3_1)$ is generated as

$$\Lambda_B(D) = \langle -f_1 + f_2, -f_2 + f_3 \rangle.$$

We are taking inner products in \mathbb{Z}^E (that is, in the basis (f_1, f_2, f_3) , so if x and y are coordinate vectors for u and v , of two elements of $\Lambda_B(D)$ expressed in the basis $(-f_1 + f_2, -f_2 + f_3)$, then

$$\langle u, v \rangle = x^\top \begin{bmatrix} 2 & -1 \\ -1 & 2 \end{bmatrix} y.$$

We call this matrix the *pairing matrix* of the lattice $\Lambda_B(D)$ with respect to the basis $(-f_1 + f_2, -f_2 + f_3)$.

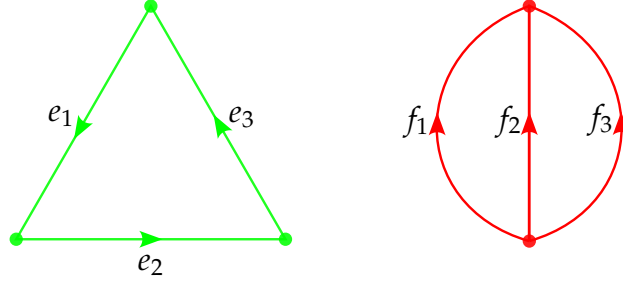


Figure 13: The Tait graphs $G_B(D)$ and $G_W(D)$.

The pairing matrix of a lattice completely describes the lattice, however the pairing matrix is not completely determined by the lattice. Instead, the lattice only determines a pairing matrix up to unimodular congruence: two matrices P and P' are *unimodular congruent* if there exists a matrix A with $\det(A) = 1$, such that $P = A^\top P' A$.

Continuing with our example, there is a single independent cycle in $G_W(D)$, it being $e_1 + e_2 + e_3$. Hence the pairing matrix of $\Lambda_W(D)$ with respect to $(e_1 + e_2 + e_3)$ is $P = [3]$.

Since the 1970's, many graph theorists have studied exactly how much information about the graph G is retained by $\Lambda(G)$ [BLN97; CV10; SW10]. In the next paragraph we see that some information about G is lost.

We call an edge e of a graph G a *bridge* if the removal of G from e disconnects G , and we say a graph G is *2-edge-connected* if G has no bridges. The lattice of integer flows of G is blind to its bridges. We define G_\bullet as G with its bridges contracted: that is, for each bridge e , we remove e and identify the adjacent vertices, then $\Lambda(G_\bullet) = \Lambda(G)$. This is because the cycles of G , and therefore the homology of G , do not see bridges.

A *2-isomorphism* between two graphs $G = (E, V)$ and $G' = (E', V')$ is a bijection $\psi : E \rightarrow E'$ which preserves cycles, i.e. $\partial(e_i + \dots + e_j) = 0$ if and only if $\partial(\psi(e_i) + \dots + \psi(e_j)) = 0$. It is well established that $\Lambda(G)$ is a 2-isomorphism invariant [BLN97]. Recent work by Su-Wagner and Caporaso-Viviani have also shown that for 2-edge-connected graphs, $\Lambda(G)$ is a complete 2-isomorphism invariant [CV10, Theorem 3.1.1; SW10, Theorem 1]. This is stated in the following theorem, which derives its name from a similar result in the context of algebraic geometry.

Theorem (Torelli Theorem for Graphs). *For two 2-edge-connected graphs G and G' , $\Lambda(G) \cong \Lambda(G')$ if and only if G and G' are 2-isomorphic.*

The notion of 2-isomorphism is completely characterised in the following way. Two graphs G and G' are related by a *Whitney flip* if it is possible to find two disjoint graphs Γ_1 (resp. Γ_2), with distinguished vertices u_1 and v_1 (respectively u_2 and v_2), such that the

identifications $u_1 = u_2 = u$ and $v_1 = v_2 = v$ form G , and the identifications $u_1 = v_2 = u'$ and $v_1 = u_2 = v'$ form G' . An example of graphs related by a Whitney flip is given in Fig. 14.

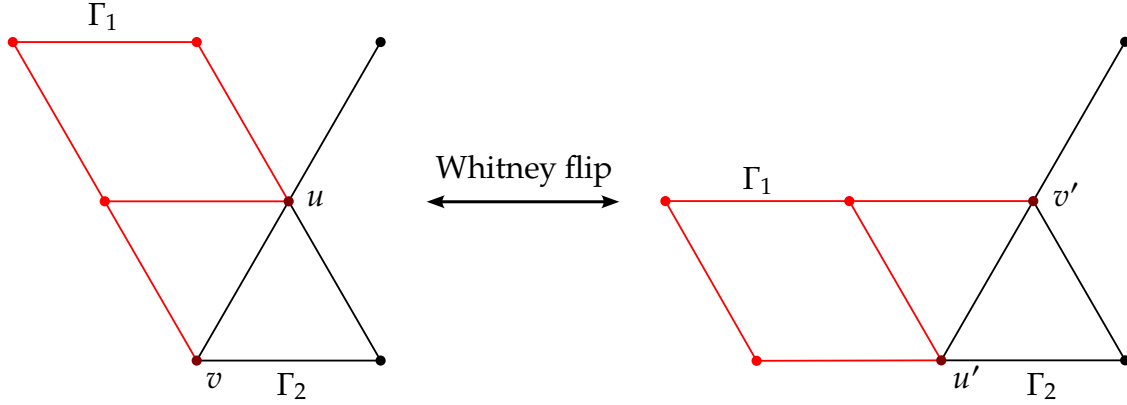


Figure 14: An example of a Whitney flip.

It is clear that sequences of Whitney flips only ever transform graphs within their 2-isomorphism class, as cycles map to cycles. From [Whi33], we have the important converse; a Reidemeister-like theorem for 2-isomorphic graphs.

Theorem (Whitney's Theorem). *Two graphs G and G' are 2-isomorphic if-and-only-if there is a sequence of Whitney flips relating G to G' .*

Our aim now is to show that $\Lambda_B(D)$ and $\Lambda_W(D)$ are invariants of alternating knots. In particular, we draw attention to the author's original geometric proof of this fact, in contrast with the topological arguments given in [Gre11].

The plan is to use the flying theorem to relate alternating diagrams of the same knot by sequences of flypes. We will discover that these translate into sequences of Whitney flips on the Tait graph. Whitney's theorem and the Torelli theorem for graphs will then relate the lattices of integer flows of the Tait graph of each diagram. The main complication will be that the flying theorem only relates alternating diagrams of prime knots. We begin with some lemmas that help us remedy this situation.

The first lemma, tells us how flypes alter the Tait graph.

Lemma. *A flype move on a knot diagram D corresponds to a Whitney flip on the Tait graph of D .*

Proof. Flipping the tangle upside down corresponds to changing the embedding of the Tait graph, but the graph itself remains unaltered. The remaining graph operation, moving the crossing in Fig. 6 to the other side corresponds to a Whitney flip with $u = v'$ and $u' = v$ being the two vertices corresponding to the coloured regions that enter either side of the tangle, and Γ_1 and Γ_2 being the two disjoint graphs formed by removing u and v , with u and v replaced. \square

The second lemma is a theorem due to Menasco [Men84], which has also been aptly paraphrased as "an alternating knot is prime if and only if it looks prime" [HTW98]:

Lemma (Menasco). *Suppose K is a knot that has an alternating diagram D . Then K is a prime knot if and only if D is a prime diagram.*

The third lemma is a textbook fact about alternating knots [Lic97].

Lemma. *Let $K = K_1 \# K_2 \# \cdots \# K_n$. Then K is alternating if and only if for all $i \in \{1, \dots, n\}$, K_i is alternating.*

The fourth lemma is a result of Kauffman, Murasugi and Thistlethwaite, a corollary of their proofs of the first Tait conjecture [Kau87; Mur87; Thi87].

Lemma (Kauffman, Murasugi, Thistlethwaite). *A reduced diagram of a prime alternating knot is alternating.*

We this, we prove that the lattice of integer flows of the Tait graph is an invariant of alternating knots.

Theorem. *Let K be alternating, and let D, E be alternating diagrams for K . Then $\Lambda_B(D) \cong \Lambda_B(E)$.*

Proof. All non-reduced alternating diagrams of K reduce to an alternating diagram for K without changing the lattice of integer flows of their Tait graphs, so we may assume that D and E are alternating reduced diagrams for K .

First we consider the case where K is a prime knot. By the flying theorem, D and E are related by a sequence of flypes. As flypes induce Whitney flips of the Tait graph, and by Whitney's theorem, $G_B(D)$ and $G_B(E)$ are 2-isomorphic. As reduced diagrams of alternating knots are 2-edge-connected, the Torelli Theorem for Graphs applies, and so $\Lambda_B(D) \cong \Lambda_B(E)$.

We also consider where K is composite. By Schubert's Theorem,

$$K = K_1 \# K_2 \# \cdots \# K_n ,$$

with each K_i prime for $i \in \{1, \dots, n\}$, and this decomposition is unique up to permutation. By the first lemma, K is composite, so D is a composite diagram:

$$D = D_1 \# D_2 \# \cdots \# D_m ,$$

for some $m > 1$. We may assume that each D_i is a prime diagram, otherwise, we could further factor the connected sum. By the second lemma, each $[D_i]$ (by this notation we mean the knot corresponding to the diagram D_i) is an alternating knot. Furthermore, again applying Menasco's theorem, we see that the knot $[D_i]$ represented by each D_i is prime. We now have two prime decompositions for K :

$$K = K_1 \# K_2 \# \cdots \# K_n ,$$

and

$$K = [D_1] \# [D_2] \# \cdots \# [D_m] .$$

By Schubert's theorem, and by relabelling the D_i , we have that $m = n$ and $[D_i] = K_i$ for each $i \in \{1, \dots, n\}$. Without loss of generality,

$$E = E_1 \# E_2 \# \cdots \# E_n ,$$

and the same is true for the E_i , hence $[D_i] = [E_i]$ for all $i \in \{1, \dots, n\}$.

We have that each $[D_i]$ or $[E_i]$ is a prime alternating knot, and each D_i or E_i is a reduced diagram, as D and E were reduced. So the theorem of Kauffman, Murasugi and Thistlethwaite gives that each D_i and E_i is an alternating diagram. For each D_i and E_i , we now have the hypothesis of the first case satisfied: we have two alternating, reduced diagrams for the same prime alternating knot, so $\Lambda_B(D_i) \cong \Lambda_B(E_i)$ for all $i \in \{1, \dots, n\}$.

Finally, since the Tait graph of a connected sum of knots is graph formed by identifying a vertex of each Tait graphs of the factor knots,

$$\begin{aligned}\Lambda_B(D) &= \Lambda_B(D_1) \oplus \Lambda_B(D_2) \oplus \dots \oplus \Lambda_B(D_n) \\ &= \Lambda_B(E_1) \oplus \Lambda_B(E_2) \oplus \dots \oplus \Lambda_B(E_n) \\ &= \Lambda_B(E).\end{aligned}$$

□

This shows that $\Lambda_B(D)$ is a well-defined function on alternating knots, and henceforth we may write $\Lambda_B(K)$ so long as K is alternating.

By the same argument $\Lambda_W(D)$ is also an invariant of alternating knots. However combining these two invariants retains no information: they are equivalent invariants to each other.

Theorem. *For alternating knots K_1 and K_2 , $\Lambda_B(K_1) \cong \Lambda_B(K_2)$ if and only if $\Lambda_W(K_1) \cong \Lambda_W(K_2)$.*

Proof. There is another lattice associated to a graph called the *lattice of integer cuts* [BLN97]. This is defined as $\text{im } \partial^*$, where $\partial^* : \mathbb{Z}^V \rightarrow \mathbb{Z}^E$ is the map adjoint to the boundary map ∂ , expressed as

$$\partial^*(v) = \sum_{e \in E} \langle \partial(e), v \rangle e.$$

The lattice of integer cuts is another integral lattice associated to G , denoted $C(G)$. We have seen already that $\Lambda(G)$ is a complete 2-isomorphism invariant, and the same is true for $C(G)$. Hence, $\Lambda(G)$ and $C(G)$ determine each other up to isomorphism.

A useful property of planar graphs G is that the lattice of integer flows of G is isomorphic to the lattice of integer cuts of G^* , that is, $\Lambda(G) \cong C(G^*)$.

Since $\Lambda_B(K_1) \cong \Lambda_B(K_2)$, we know that $C_B(K_1) \cong C_B(K_2)$. But $C_B(K_i) \cong \Lambda_W(K_i)$, for $i \in \{1, 2\}$, and the result follows. □

The statement that $\Lambda(G) \cong C(G^*)$ is true only for planar graphs, and when we later consider a surface-dual version of this theory, the first homology of the surface will play a role.

It only remains to show that $\Lambda_B(K)$ is a complete invariant up to mutation. The following lemma examines the effect of mutation on the Tait graph [Gre11, Lemma 4.5]:

Lemma (Greene). *Depending on the tangle to be mutated, a mutation of D either:*

- *affects only the planar embedding of the Tait graph, leaving its graph structure unchanged, or*
- *induces a Whitney flip in the Tait graph.*

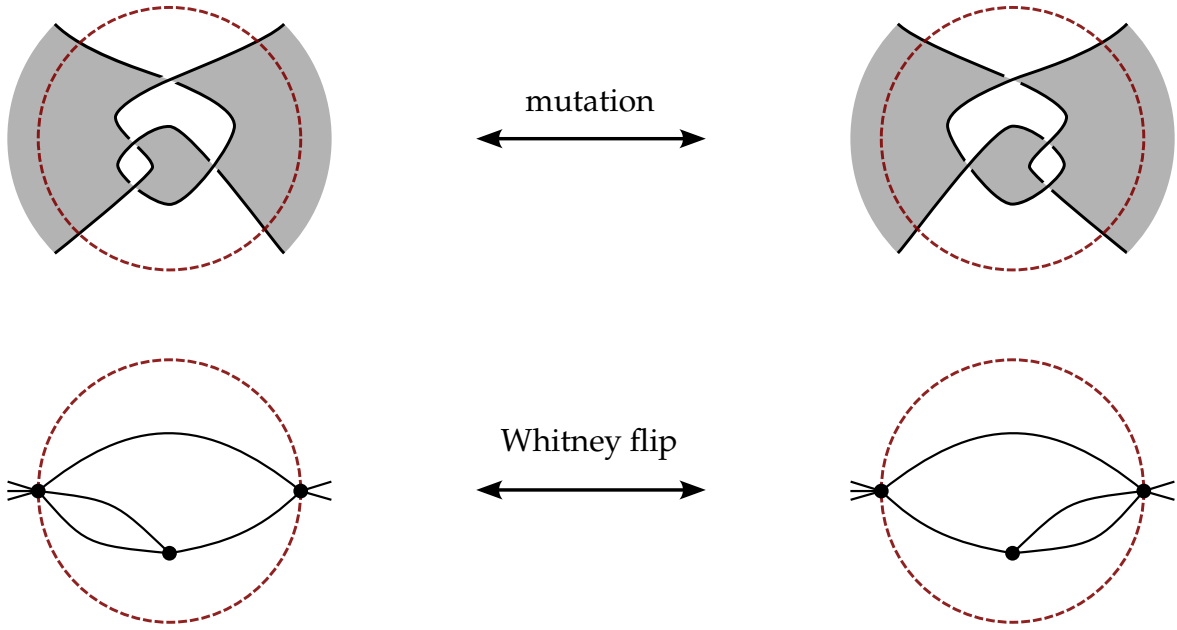


Figure 15: A mutation may induce a Whitney flip. Figure modified from [Gre11, Fig. 2].

Conversely, a Whitney flip in the Tait graph induces a mutation in D .

A single case in the proof of this lemma can be found in Fig. 15. For the full proof including remaining cases consult [Gre11, Fig. 2-4]. Greene uses this lemma to prove that the lattice of integer flows of the Tait graph is a complete mutation invariant of alternating knots [Gre11, Proposition 4.4].

Theorem (Greene). *Let K_1 and K_2 be alternating knots. Then K_1 and K_2 are mutants if and only if $\Lambda_B(K_1) \cong \Lambda_B(K_2)$.*

Proof. Let K_1 and K_2 be alternating knots. For the forward implication, suppose that K_1 and K_2 are mutants, so there is a sequence of mutations from a diagram of K_1 to a diagram of K_2 . By the lemma above, their Tait graphs $G_B(K_1)$ and $G_B(K_2)$ are related by Whitney flips. By Whitney's theorem, each of these pairs of graphs are 2-isomorphic. Since $\Lambda_B(G)$ is a 2-isomorphism invariant, $\Lambda_B(K_1) \cong \Lambda_B(K_2)$.

For the reverse implication, take two alternating knots such that $\Lambda_B(K_1) \cong \Lambda_B(K_2)$. We may assume them to be reduced, as reduction of a knot does not alter the lattice of integer flows of its Tait graphs. As the knots are reduced, their Tait graphs are 2-edge-connected. So, by the Torelli theorem for graphs, $G_B(K_1)$ and $G_B(K_2)$ are 2-isomorphic. By Whitney's theorem, there is a sequence of Whitney flips between each of these pairs, which by the lemma above corresponds to a sequence of mutations between K_1 and K_2 , so they are mutants. \square

1.5 Heegaard-Floer Homology and the d -invariant

Greene shows that the lattice of integer flows of a graph can be reduced into an equivalent, more concise invariant called the d -invariant. When this is applied to the Tait graph of a

knot, we refer to it as the ‘lattice-theoretic’ d -invariant. Greene shows that this invariant coincides with a construction from Heegaard-Floer homology, known as the d -invariant of the Heegaard-Floer homology of the double branched-cover of the knot, which we refer to as the ‘Heegaard-Floer’ d -invariant [Gre11].

Heegaard-Floer homology is a homology theory introduced in a series of papers by Peter Ozsváth and Zoltan Szábo [OS05; OS03; OS04] at the turn of the 21st century. The theory consists of a powerful set of topological invariants that fit within a topological quantum field theory. This framework has proven to be incredibly useful in low-dimensional topology; a good overview is [Gre21]. In this text we work predominantly with the lattice of integer flows, but we include a brief introduction to the d -invariant below.

The *dual lattice* of an arbitrary lattice Λ is the rational lattice

$$\Lambda^* = \left\{ x \in \Lambda \otimes \mathbb{Q} \mid \langle x, \lambda \rangle \in \mathbb{Z}, \forall \lambda \in \Lambda \right\}$$

To construct the d -invariant, Greene shows that instead of considering the whole lattice $\Lambda_B(K)$, it suffices to look at a particular coset in $\Lambda^*/2\Lambda^*$ called the *characteristic coset*:

$$\text{Char } \Lambda = \left\{ \chi \in \Lambda^* \mid \langle \chi, \lambda \rangle \equiv \langle \lambda, \lambda \rangle \pmod{2} \forall \lambda \in \Lambda \right\}.$$

The d -invariant is a scaled mapping taking a coset of covectors $[\chi]$ in $\text{Char}(\Lambda) \pmod{2\Lambda}$ to a scaled version of the minimal norm of all $\chi \in [\chi]$.

In my computational work, I implemented code to compute both $\Lambda_B(K)/\Lambda_W(K)$ and the d -invariant for all tabulated alternating virtual knots.

Chapter 2

Virtual Knots

*I thought this was the end
But no my friends, this is when
We get to do it all again...*

— The Muppets, *We're Doing a Sequel*

...and now it's virtual...

— Jamiroquai, *Virtual Insanity*

We now introduce the exciting and relatively new theory of virtual knots. Virtual knots are a generalisation of knots, and there are many different equivalent formulations of them. We start with the most geometric of the formulations, but we also present a combinatorial definition of computational significance later.

2.1 Knots in Thickened Surfaces

In this section we will largely follow the work of Kuperberg [Kup03] and Carter-Kamada-Saito [CKS00] and give the geometric definition of virtual knots as knots in thickened surfaces.

Classical knots, a term which refers specifically to the kind of knots we have introduced in Chapter 1, are represented by diagrams in the plane, \mathbb{R}^2 , but really they have an extra dimension of ‘thickness’, encoded in the diagram by the under- and over- crossings. That is, knots are embeddings of a circle in the “thickened plane”, in other words \mathbb{R}^3 . However, we didn’t really need a whole \mathbb{R} ’s worth of extra space. We could easily think of classical knots as living in a thickened plane, $\mathbb{R}^2 \times I$ where I is the unit interval $[0, 1]$. Thinking of knots as embeddings in $\mathbb{R}^2 \times I$, it becomes natural to ask: what if we replace the plane by another surface; can we draw diagrams on other surfaces Σ and therefore knots in *thickened surfaces* $\Sigma \times I$? The answer to these questions is yes, and virtual knots are one such generalisation.

In the context of virtual knots, all surfaces of relevance are closed and orientable. Note that classical knots fit into this picture, as knot diagrams on the plane are equivalent to knot diagrams on the sphere. The only extra move allowed by this one-point compactification is that a strand on one side of a knot diagram can be taken over to the other by spherical

isotopy of moving it around the back side of the sphere. However this was already allowed on the plane by a sequence of *RIII* and *RII* moves.

There is a well-known classification theorem for closed, orientable surfaces as follows.

Theorem (Classification of compact, orientable surfaces). *Each connected component of a compact, orientable surface is homeomorphic to:*

- the sphere, \mathbb{S}^2 , or
- a connected sum of g tori, $g\mathbb{T}^2$, for $g \geq 1$.

Hence there is a bijection between connected components of compact, orientable surfaces and the natural numbers given by the *genus*, g of the surface: the number of handles.

A *surface knot diagram* on Σ is the analogue of a classical knot diagram, but drawn on a closed, oriented, connected surface, Σ , which is no longer necessarily the plane. The equivalence relation on surface knot diagrams is given by the Reidemeister moves and surface isotopy (the surface-analogue of planar isotopy) on Σ .

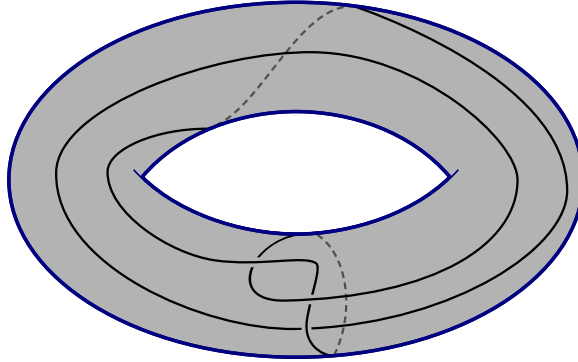


Figure 16: A surface knot diagram on $\Sigma = \mathbb{T}^2$.

Instead of drawing surface knot diagrams directly on compact orientable surfaces, for genus $g \geq 1$, we often draw on the gluing diagrams of those surfaces. From a textbook theorem of algebraic topology [Hat00, Chapter 0], the compact orientable surface of genus g is obtained from the $4g$ -gon by gluing around the polygon with the pattern $aba^{-1}b^{-1}, cdc^{-1}d^{-1}, \dots$ continuing on for g iterations, that is, until all edges have been glued. Fig. 17 shows gluing diagrams for \mathbb{T}^2 and $2\mathbb{T}^2$.

Knots in thickened surfaces relate to surface knot diagrams, in the same way knots and knot diagrams are related in the classical context. A *knot in a thickened surface* $\Sigma \times I$ is an embedding $K : S^1 \hookrightarrow \Sigma \times I$ up to ambient isotopy in $\Sigma \times I$. We denote a knot K in thickened surface $\Sigma \times I$ as (K, Σ) . The diagram of K is a projection of K onto Σ with under- and over-crossings.

We say a surface knot diagram is *cellularly embedded* if $\Sigma \setminus D$ is a union of disks. Being cellularly embedded is a way to check that a knot ‘fully utilises’ the surface it is drawn on, in the following sense. Observe that the surface knot diagrams in Fig. 17b and Fig. 17c are cellularly embedded, and in fact, these surface knot diagrams could not be drawn on a surface of lower genus. If, for example, one was to try draw the surface knot diagram

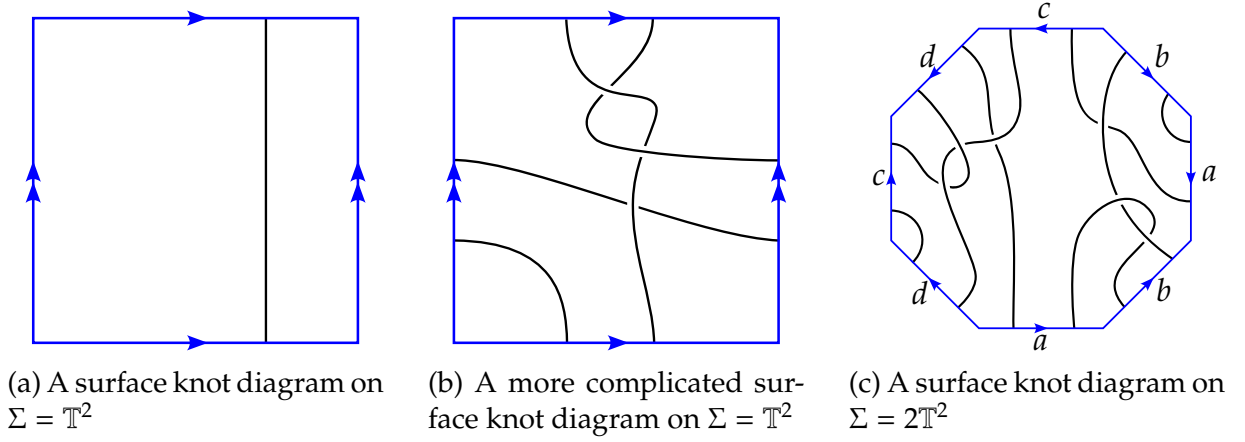


Figure 17: Some examples of surface knot diagrams. Note that classical knot diagrams would also be examples with $\Sigma = S^2$.

in Fig. 17b on the plane, connecting the four pairs of loose ends at the sides would not be possible without introducing additional crossings. In contrast, the surface knot diagram in Fig. 17a represents the unknot drawn as a homologically non-trivial curve on the torus. This could be drawn on the plane/sphere, however we don't yet have a notion of equivalence for surface knot diagrams (or knots in thickened surfaces) that live on surfaces of different genus.

Note that while a non-cellularly-embedded diagram could be drawn on a surface of lower genus, the converse does not hold: a knot that is cellularly embedded might still be able to be drawn on a diagram of lower genus, such as in Fig. 18. These examples motivate the definition of stable equivalence in the next section.

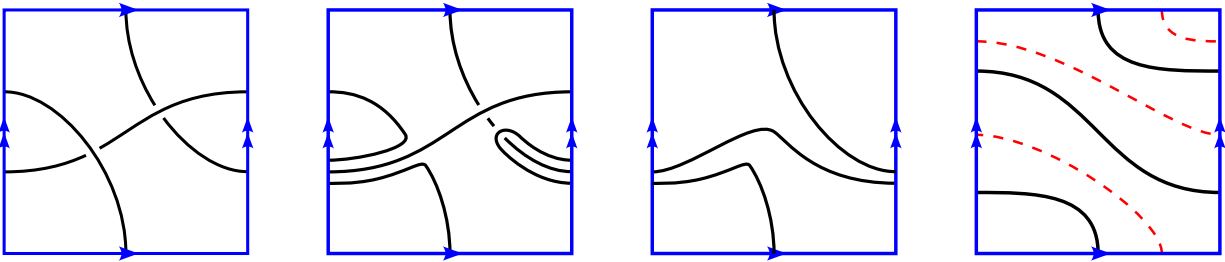


Figure 18: An example of surface knot diagram which transforms to a not-cellularly-embedded diagram only after some Reidemeister moves. The single face in the final diagram contains a non-homologically-trivial cycle, marked in red, and hence is not contractible (not a disk).

2.2 Stable Equivalence and Virtual Knots

Virtual knots are knots in thickened surfaces of any genus modulo the equivalence relation of stable equivalence. We give the definition on the level of surface knot diagrams, but it can be stated equivalently for embeddings $K \hookrightarrow R \times I$.

The operation of *stabilisation* is defined as follows: find two disks B_1 and B_2 in Σ that do not intersect D , remove B_1 and B_2 from Σ and then glue a handle whose boundary is $B_1 \cup B_2$. Intuitively, stabilisation is ‘adding a handle’ to Σ , and any newly added handle does not interact with P .

The reverse operation *destabilisation* is defined as follows: Take a cylinder Y that does not intersect D , and such Y does not deformation-retract to not a null-homologous circle. Removes the Y , and glue a cap to both resulting boundary circles.

The point of stable equivalence is to identify two knot diagrams D_1 and D_2 that would otherwise be identical, except for living on surfaces Σ_1 and Σ_2 of different genus as in the example above.

Hence we define a *virtual knot* as an equivalence class of knots in thickened surfaces under stable equivalence. Two surface knot diagrams represent the same virtual knot if there is some sequence of Reidemeister moves and stabilisation/destabilisation moves from one diagram to the other.

For a virtual knot we use the notation V , but when referring to knots in thickened surfaces (such as specific representatives of virtual knots), we use (K, Σ) . That is, we use V when the object is being considered up to stable equivalence and K otherwise.

The *virtual genus* g_v of a virtual knot V is defined as the minimum genus of all surface knot diagrams for V . The virtual knots with virtual genus $g_v = 0$ are classical knots, and the virtual knots with virtual genus $g_v > 0$ are *strictly virtual*. The virtual knots in Fig. 17b and 17c are examples of strictly virtual knots.

An important question to ask is whether classical knot theory embeds faithfully into virtual knot theory: are there distinct classical knots which, when considered as virtual knots are rendered equivalent by stable equivalence? A uniqueness result of Kuperberg dispels this possibility and in fact gives the even stronger result that we *never* need to go ‘up’ in genus to check whether virtual knots are equivalent.

Theorem (Kuperberg’s Theorem). *If (K, Σ) and (J, Σ) are two minimal genus representatives of the same virtual knot of virtual genus g_v , then they are equivalent as knots $\Sigma \times I$. That is, there is a self-diffeomorphism φ of $\Sigma \times I$ such that $\varphi(K) = J$.*

However, as we illustrated in Fig. 18, the virtual genus of a virtual knot is not necessarily obvious, and furthermore, there is no known algorithm to compute it. The following theorem from [Man13], does allow for the computation of g_v for low crossing numbers:

Theorem (Manturov). *If a diagram of a knot K in a thickened surface $\Sigma \times I$ contains the minimal number of crossings across all diagrams in thickened surfaces, then Σ is the minimal genus surface that can support K . That is, the genus of Σ is the knot’s virtual genus.*

In combination with Kuperberg’s theorem, this says we also never need to go increase the genus of the supporting surface to reduce crossing number. It suffices to reduce the genus as much as possible, and then perform Reidemeister moves.

2.3 Diagrams with Virtual Crossings

We take a short detour to relate knots in thickened surfaces modulo stabilisation to an equivalent combinatorial definition of virtual knots. This is, in fact, the original formula-

tion of virtual knots, due to Kauffman [Kau99]. Given a diagram of a knot K on a surface Σ , we obtain a diagram of K on the plane by embedding Σ in \mathbb{R}^3 then projecting down to \mathbb{R}^2 . Doing so creates a new type of crossing, which did not exist on Σ , but is an artefact of the projection. We call these crossings virtual crossings. Those crossings coming from a crossing on Σ , we call *classical crossings*, and they have the usual over- and under-stands as determined by the projection. For strictly virtual knots these virtual crossings are necessary, as the knot diagram as a 4-valent graph is not planar.

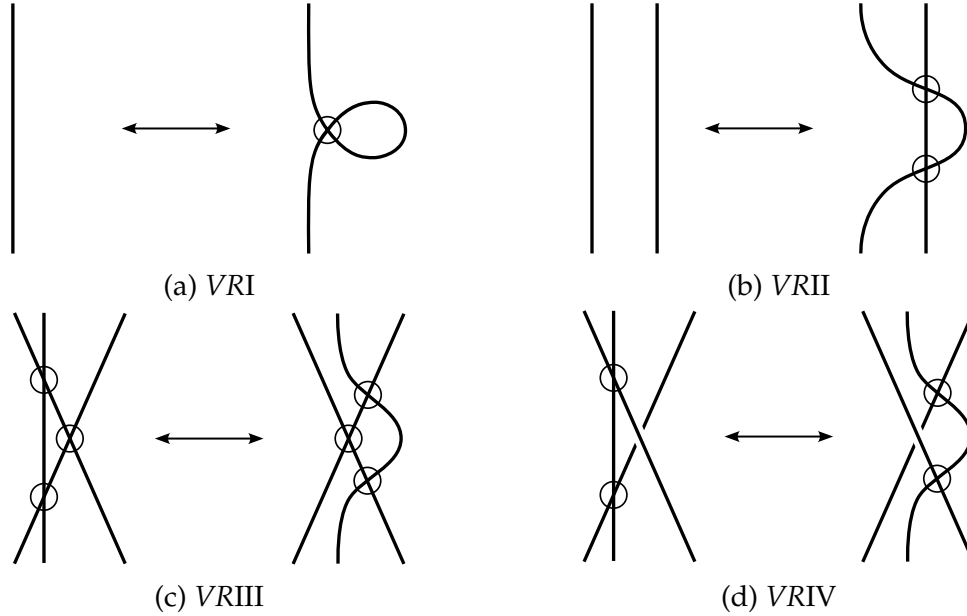


Figure 19: The four additional virtual Reidemeister moves.

The relevant equivalence relation on diagrams with virtual crossings are not hard to deduce. The three Reidemeister moves which hold between classical crossings, there are three corresponding with virtual crossings, and finally a ‘triangle move’ that moves a ‘virtual strand’ through a crossing. These additional moves are shown in Fig. 19.

Classification efforts for virtual knots follow a similar strategy as for classical knots. The current best tabulation is by Jeremy Green [Gre04], up to 6 crossings. Green achieved this by computing all possible virtual knot diagrams up to 6 crossings, determining which are equivalent via virtual Reidemeister moves, and then computing enough invariants distinguish all of these knots.

Since the virtual knot diagrams in Green’s tabulation are by construction minimal crossing representations, by Manturov’s theorem, this allows for the computation of virtual genus for all tabulated virtual knots. In Green’s tabulation virtual knots are presented using yet another representation: Gauss codes. Gauss codes are a concise way of encoding the information of a virtual knot diagram in a discrete computationally useful format. We introduce them in Chapter 4.

2.4 Annular Connected Sums and Prime Virtual Knots

The rest of this chapter is aimed at constructing invariants of alternating virtual knots. We do this from the perspective of the lattices of integer flows of the Tait graphs of the virtual knot rather than equivalent d -invariant formulation of [Gre11]. But first we, introduce the tools used in Chapter 1 in the new virtual setting, starting with connected sums. We work with the definition of virtual knots as knots in thickened surfaces under stable equivalence.

We define connected sums for knots in thickened surfaces. We need to give a definition which plays well with stable equivalence, that is, connected sums of stabilised knots on thickened surfaces remain stabilised.

First, we must define connected sums for close orientable surfaces. The *connected sum* of Σ_1 and Σ_2 is the surface $\Sigma_1 \# \Sigma_2$, obtained by removing a disk each from Σ_1 and Σ_2 , then gluing together the resulting boundary circles. As this operation does not introduce or remove handles, $g(\Sigma_1 \# \Sigma_2) = g(\Sigma_1) + g(\Sigma_2)$.

To define annular connected sums for surface knot diagrams, begin with the following: for $i \in \{1, 2\}$, a surface knot diagram (D_i, Σ_i) and representing knot (K_i, Σ_i) and a disk B_i in Σ_i that intersects D_i transversely at two points, and $D_i \cap B_i$ is unknotted relative to ∂B_i – see Fig. 20. Then, the *annular connected sum* $(D, \Sigma) = (D_1, \Sigma_1) \#_{B_1, B_2} (D_2, \Sigma_2)$ is constructed by gluing B_1 and B_2 such that the two element set $\partial B_1 \cup D_1$ is glued to an element of $\partial B_2 \cap D_2$.

We say that $(K, \Sigma) = (K_1, \Sigma_1) \# (K_2, \Sigma_2)$. Unlike in the classical case, this is not in general well-defined [KM06], and depends on both the surface diagrams for K_1 and K_2 and the chosen disks. However, if $\Sigma_1 = \Sigma_2 = \mathbb{S}^2$, then this definition is equivalent to the connected sum of classical knots, and well-defined. In general, we write $(K_1, \Sigma_1) \# (K_2, \Sigma_2)$ for any of the annular connected sums of (K_1, Σ_1) and (K_2, Σ_2) .

An annular connected sum where one of the summands is the unknot in $\mathbb{S}^2 \times I$ the sum is said to be *trivial*. A knot in a thickened surface is *prime* if it is not the non-trivial annular connected sum of any two knots in thickened surfaces.

The *connected sum* of two virtual knots is the annular connected sum of their surface diagram. This again depends both on the representatives and the disks chosen in the annular connected sum.

A connected sum of virtual knots $V = V_1 \# V_2$ is *trivial* if one of the summands is in the stable equivalence class of the unknot in $\mathbb{S}^2 \times I$, and the other is equivalent to V . A virtual knot (other than the trivial knot) is *prime* if there is no way to write it as a non-trivial connected sum.

Despite the ill-defined nature of the annular connected sum, the decomposition of virtual knots into their constituent primes behaves in a nice way on a certain subset of all virtual knots. The theorem analogous to Schubert's theorem in the virtual setting is a result of Matveev [Mat12, Theorem 13].

Theorem (Matveev's Theorem). *Any virtual knot can be decomposed into a connected sum of prime and trivial virtual knots. The prime summands in this decomposition are determined uniquely, that is, depend only on the initial virtual knot.*

There is also a notion of *weakly prime* virtual knots which cannot be decomposed as a connected sum of one virtual and one classical knot. The formal definition is given by

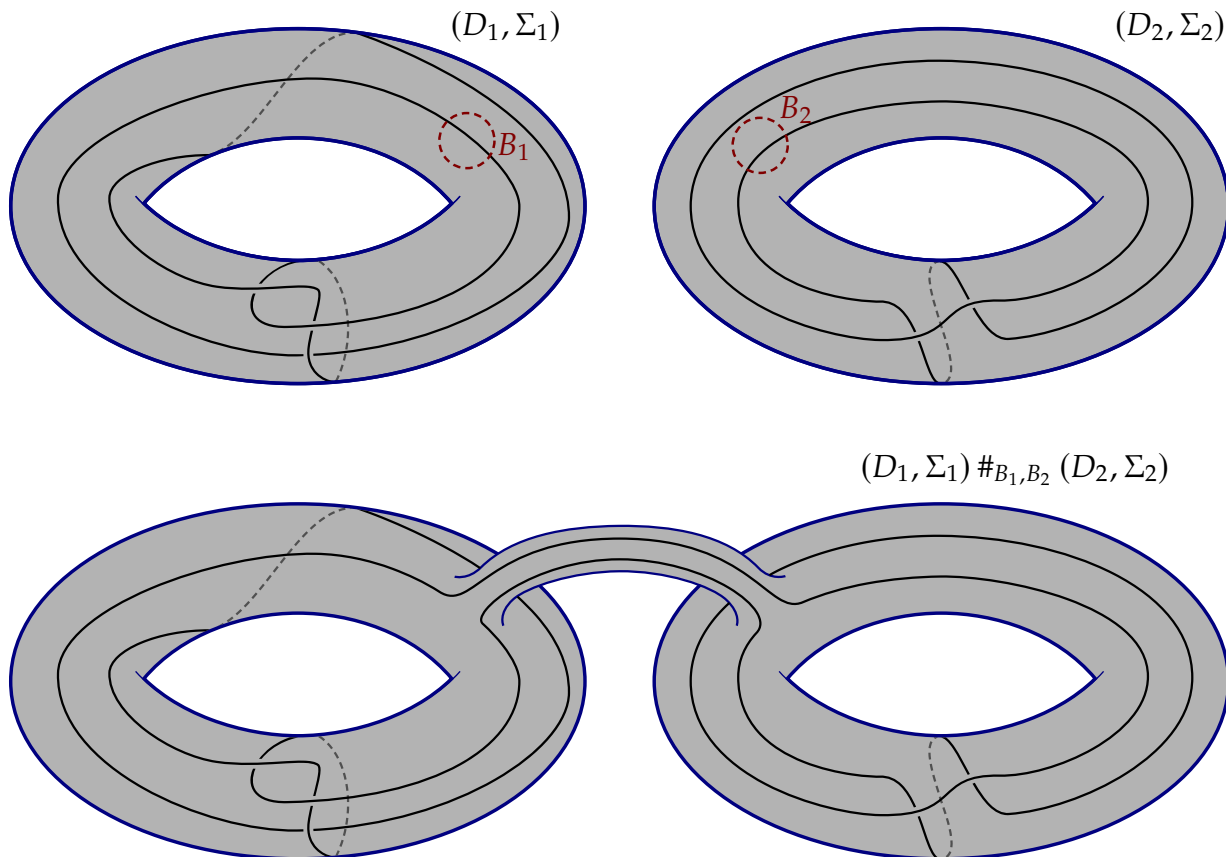


Figure 20: A (but not the only) example of an annular connected sum of (K_1, Σ_1) and (K_2, Σ_2) with respect to the diagrams (D_1, Σ_1) and (D_2, Σ_2) shown. The knots in thickened surfaces are representatives of virtual knots 3_7 and 2_1 .

Howie-Purcell [HP17].

2.5 Alternating Virtual Knots and Virtual Knot Mutation

A famous theorem Seifert in classical knot theory states that It is always possible to find some orientable surface $S \subseteq \mathbb{R}^3$ called the Seifert surface, such that $\partial S = K$. There is a vast amount of theory that springs from this fact, and Chapters 3 and 4 will examine a generalisation of a small amount of this. Virtual knots which do possess Seifert surfaces behave so classically that they are called *almost classical*, but only a small fraction of strictly virtual knots have this property.

For virtual knots, it is not usually possible to find such a surface inside $\Sigma \times I$. Indeed typically it is not even possible to find a non-orientable surface with boundary V . Those virtual knots for which this is possible are exactly those that are \mathbb{Z}_2 -null-homologous, and we will look at these in the next section. A further subset of these knots are *alternating*, where alternating has the same definition as in the classical case.

Alternating virtual knots maintain many of the properties of alternating classical knots.

For example, Greene’s characterisation as knots with positive definite and negative definite spanning surfaces generalises to the virtual setting [BK23a].

Alternating knots are also important because virtual analogues of the Tait conjectures hold. The first Tait conjecture was recently proven for virtual knots by Karimi [Kar18, Theorem 1.6]:

Theorem (First Tait Conjecture for Virtual Knots). *Let D be a reduced alternating knot diagram for a virtual knot V . Then D has minimal crossing number.*

Very recent work of Kindred also shows that for weakly prime virtual knots the third Tait conjecture holds [Kin22, Theorem 4.18]:

Theorem (Virtual Flying Theorem). *Let (K, Σ) be a knot in a thickened surface. Let D and E be weakly prime, alternating, cellularly embedded surface diagrams of K . Then D and E are related by a sequence of flypes on Σ .*

There are two types of mutation of virtual knots: disk mutation and surface mutation. *Disk mutation* is directly analogous to mutation of classical knots: take a disk $D \subseteq \Sigma$ which contains a tangle and flip or rotate it, the resulting knot is a disk mutant of the original. This is in contrast to *surface mutation*, in which the chosen subsurface need only have circular boundary, but could contain handles. Surface mutation is a more invasive operation and we do not consider it in the present text. However, future work may lie in investigating the equivalence classes generated by surface mutation. For the rest of this text, mutation, in the virtual context, refers to disk mutation.

2.6 Checkerboard Colourings and Tait Graphs of Virtual Knots

Recall that in the classical case, all knots are checkerboard colourable, so there is no obstruction to producing Tait graphs. Furthermore, only one Tait graph is necessary to encode an alternating knot, as the two Tait graphs are planar duals to each other. We will see that the virtual case is more subtle.

Not all surface knot diagrams are checkerboard colourable. Worse, any checkerboard colourable diagram on a surface Σ can be made non-checkerboard colourable by adding a handle: see Fig. 21. Adding a handle between a black region and a white region creates a region needing to be both black and white, so the diagram on the stabilised surface is not checkerboard colourable.

We say a knot in a given thickened surface $\Sigma \times I$ is *checkerboard colourable* if there exists a checkerboard colourable surface knot diagram on Σ that represents it. We have the following classification of checkerboard colourable knots in thickened surfaces [BK19]:

Theorem. *Given a knot in a thickened surface, $K \subset \Sigma \times I$, the following are equivalent:*

- (i) K is checkerboard colourable,
- (ii) K is the boundary of an unoriented spanning surface $F \subset \Sigma \times I$,
- (iii) $[K] = 0$ in the homology group $H_1(\Sigma \times I; \mathbb{Z}_2)$.

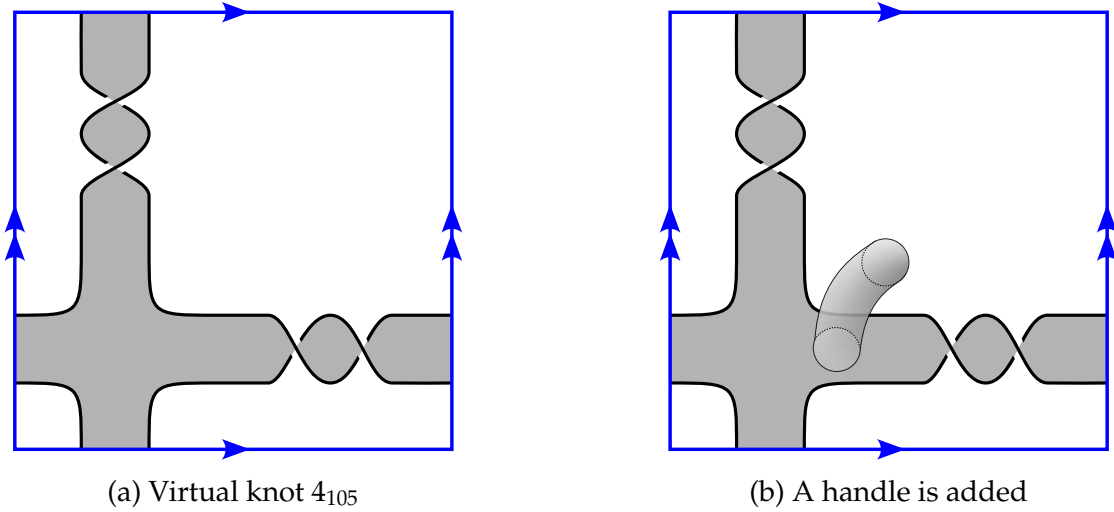


Figure 21: Adding a handle can disrupt checkerboard colourability.

Likewise, we say a virtual knot is *checkerboard colourable* if there is a representative that is checkerboard colourable. Note that while the knot in a Fig. 21b isn't checkerboard colourable as a knot in a $2\mathbb{T}^2 \times I$, it is indeed checkerboard colourable as a virtual knot, as after destabilisation we have the knot in Fig. 21a. Not every virtual knot is checkerboard colourable, even on its surface of minimal genus: see Fig. 22.

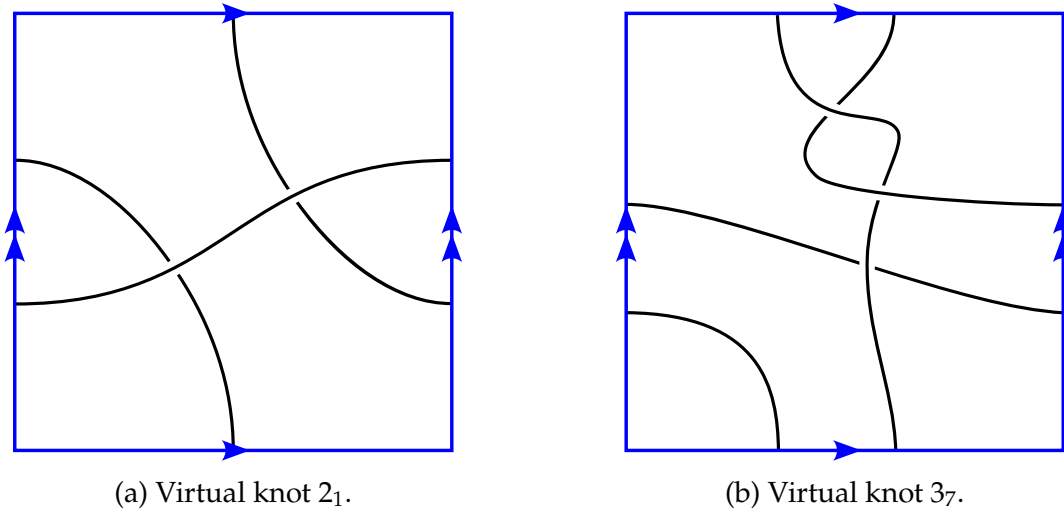


Figure 22: Two virtual knots on their surfaces of minimal genus. The knot 2_1 is not checkerboard colourable in the given diagram. In fact 2_1 is not checkerboard colourable at all, as $[K] \neq 0$ in $H_1(\Sigma \times I; \mathbb{Z}_2)$. The knot 3_7 is checkerboard colourable.

For the purposes of generalising the lattice of integer flows of the Tait graph, we need only concern ourselves with alternating virtual knots – those virtual knots that can be represented by alternating virtual knot diagrams. Fortunately, tanks to the following theorem will not run into any trouble [Kam02, Lemma 7].

Theorem (Kamada’s Lemma). *Every alternating virtual knot is checkerboard colourable.*

Furthermore, just as in the classical case, alternating surface knot diagrams have the property that when checkerboard coloured, all crossings have the same type [BK23a, Lemma 6]. Again, the convention is to choose the checkerboard colouring such that all crossings are type A (see Fig. 11).

For those surface knot diagrams that are checkerboard colourable, we can define the Tait graphs of the knot. In the classical case, these were planar graphs, or more specifically planar embedded graphs. In the virtual context, they are surface embeddings.

Let G be a connected graph. A *surface embedding* of G is a map $i : G \hookrightarrow \Sigma$, considered up to orientation-preserving diffeomorphism. To simplify notation, we use G and $i(G)$ interchangeably.

A *cellular embedding* of a graph is a surface embedding $i : G \hookrightarrow \Sigma$ such that $\Sigma \setminus G$ is a union of disks. Given a cellular embedding of a graph G in an orientable surface, we can read off a cyclic ordering of incident edges around each vertex. In fact, a textbook result in topological graph theory is that a cyclic ordering of incident edges around each vertex uniquely determines a cellular surface embedding for G [MT01, Theorem 3.2.4]. This extra information is called a *rotation system*; a graph with a rotation system is also called a *ribbon graph* or *fat graph*.

The *surface dual* of the cellularly embedded surface graph $i : G \hookrightarrow \Sigma$ is another surface embedding $i^* : G^* \hookrightarrow \Sigma$, where G^* is the graph that has a vertex for every connected component of $\Sigma \setminus G$, and for each edge e of G , a dual edge e^* connecting the vertices lying on either side of e .

The following elementary results justify the definition of surface duals.

Lemma. *Let G be cellularly embedded. Then G^* is cellularly embedded.*

Proof. Since G is cellularly embedded in Σ , the Euler characteristic $\chi(\Sigma) = |V(G)| - |E(G)| + |F(G)|$. From the definition of the surface dual, $|V(G^*)| = |F(G)|$ and $|E(G^*)| = |E(G)|$. Now let v denote an arbitrary vertex of G . Consider the set of edges dual to the edges incident to v . This forms a cycle in G^* which separates v from all other vertices. Since there are no other edges inside this cycle, it is a face containing only the vertex v . Hence, $|F(G^*)| \leq |V(G)|$. Conversely each connected component of $\Sigma \setminus G^*$ is bounded by a cycle of at least one edge, e^* . The edge e dual to e^* terminated within the connected component $\Sigma \setminus G^*$, so this component or ‘face’ must contain a vertex, so $|F(G^*)| \geq |V(G)|$. Hence, the Euler characteristic $\chi(G^*) = \chi(G)$, so G^* is also cellularly embedded. \square

Corollary. *If G is cellularly embedded, then $G^{**} = G$.*

Like in the classical case, we can reconstruct the knot diagram of an alternating virtual knot from a cellular embedding of the Tait graph. Since the faces of the Tait graph are disks in a cellular embedding, the construction is completely analogous to the classical case, as shown in Fig. 12.

2.7 The Lattice of Integer Flows for Virtual Knots

This section will be dedicated to determining whether the results about the lattice of integer flows in the classical case generalise to the virtual setting. Like the classical case,

we find that the lattice of integer flows of either Tait graph of a virtual knot is an invariant of alternating virtual knots. However, the proof that this is a *complete* invariant fails for alternating virtual knots. In fact, in Chapter 4, we will produce a counterexample.

As the lattice of integer flows is defined graph-theoretically, the same definition applies in the virtual setting. The difference is that embedded black and white Tait graphs are no longer planar duals, but surface duals. As a result, the lattice of integer flows of the white Tait graph is no longer isomorphic to the lattice of integer cuts of the black Tait graph, so both $\Lambda_B(D)$ and $\Lambda_W(D)$ are needed to retain as much information as possible. We present the following example to illustrate this.

Let $K = 5_{2429}$, and D the surface knot diagram given in Fig. 23a. The Tait graphs are given abstractly in Fig. 24.

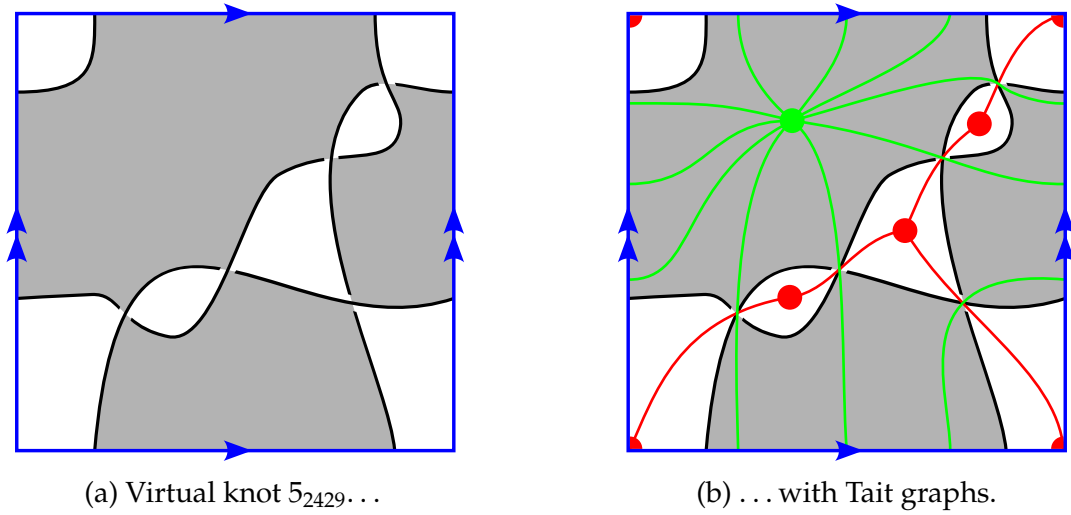


Figure 23

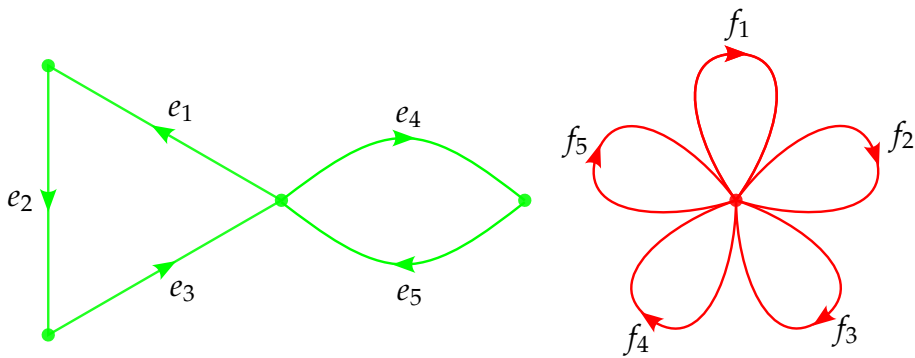


Figure 24: The Tait graphs $G_B(D)$ and $G_W(D)$.

With respect to the basis $(e_1 + e_2 + e_3, e_4 + e_5)$, the inner product on $\Lambda_B(D)$ has pairing matrix

$$\begin{bmatrix} 3 & 0 \\ 0 & 3 \end{bmatrix}.$$

Likewise with respect to the basis $(f_1, f_2, f_3, f_4, f_5)$, $\Lambda_W(D)$ has pairing matrix

$$\begin{bmatrix} 1 & 0 & 0 & 0 & 0 \\ 0 & 1 & 0 & 0 & 0 \\ 0 & 0 & 1 & 0 & 0 \\ 0 & 0 & 0 & 1 & 0 \\ 0 & 0 & 0 & 0 & 1 \end{bmatrix}.$$

Again, these pairing matrices are only determined by the lattices up to unimodular congruence. To contrast the classical case, we also look at the lattice of integer flows of $G_W(D)$ and $G_B(D)$: the lattice $C_B(D)$ with respect to the basis $(e_1 - e_2, e_2 - e_3, e_4 - e_5)$ has pairing matrix with pairing matrix

$$\begin{bmatrix} 2 & -1 & 0 \\ -1 & 2 & 0 \\ 0 & 0 & 2 \end{bmatrix},$$

and the lattice $C_W(D)$ is the lattice $\{0\}$.

In the classical case, the lattice of integer cuts of G_W is isomorphic to the lattice of integer flows of G_B : $\Lambda_B(G) \cong C_W(G)$, and vice-versa. In the virtual case, we see that this is no longer true - their pairing matrices are not even the same dimension.

In the classical setting, to prove that $\Lambda_B(D)$ and $\Lambda_W(D)$ are invariants of alternating knots, we used the flying theorem to relate any prime alternating diagrams via a sequence of flypes. Then, by the lemma that flypes correspond to Whitney flips of the Tait graph, any two prime alternating diagrams of the same knot have isomorphic lattices. Finally we use a series of results to extend this from prime alternating knots to arbitrary alternating knots, including Menasco's theorem and the unique decomposition theorem (Schubert's theorem) for knots.

The virtual case is more complicated. Kindred's virtual flying theorem applies to weakly prime alternating knots, and virtual analogues of results used in the classical proof are weaker and more subtle.

Therefore, for virtual knots, we give a different topological proof for the invariance of $\Lambda_B(D)$ and $\Lambda_W(D)$ by showing that the lattice of integer flows of the Tait graph is equivalent to the topologically defined Gordon-Litherland pairing. We state this now, but delay the proof to Chapter 3, where we introduce the Gordon-Litherland pairing.

Theorem. *Let V be an alternating virtual knot, and let D, E be reduced, alternating, cellularly embedded surface knot diagrams for V . Then $\Lambda_B(D) \cong \Lambda_B(E)$ and $\Lambda_B(D) \cong \Lambda_W(E)$.*

Two statements from the classical case remain to be examined: that $\Lambda_B(V)$ (resp. $\Lambda_W(V)$) is a mutation invariant, and that $\Lambda_B(V)$ (resp. $\Lambda_W(V)$) is complete up to mutation. The first statement holds in the virtual setting.

Theorem. *Let V_1 and V_2 be mutant alternating knots that are mutants. Then $\Lambda_B(V_1) \cong \Lambda_B(V_2)$ and $\Lambda_W(V_1) \cong \Lambda_W(V_2)$.*

Proof. The proof follows the proof in the classical case exactly. Let V_1 and V_2 be mutants. There is a sequence of mutations from V_1 to V_2 . The lemma from Chapter 1 that a flype

move induces a Whitney flip of the Tait graph generalises directly to disk mutation. Thus, $G_B(V_1)$ and $G_W(V_1)$ (resp. $G_B(V_2)$ and $G_W(V_2)$) are related by Whitney flips. By Whitney's theorem, the graphs are 2-isomorphic, and since $\Lambda_B(K)$ (resp. $\Lambda_W(K)$) is a 2-isomorphism invariant, we have $\Lambda_B(V_1) \cong \Lambda_B(V_2)$ (resp. $\Lambda_W(V_1) \cong \Lambda_W(V_2)$). \square

However the proof of completeness fails to generalise: let (D_1, Σ_1) and (D_2, Σ_2) be alternating diagrams of virtual knots such that $\Lambda_B(D_1) \cong \Lambda_B(D_2)$. Like in the classical case, the discrete Torelli theorem applies, so the abstract graphs $G_B(D_1)$ and $G_B(D_2)$ are determined up to 2-isomorphism by the lattice of integer flows. Unlike in the classical case, due to the variety of different homology classes edges can be embedded in, not all of the ways of embedding $G_B(D_1)$ and $G_B(D_2)$ are reachable from each other by Whitney flips. For example, a Whitney flip can never take a homologically non-trivial cycle to a homologically trivial cycle, or vice-versa.

In fact, on the class of virtual knots, even the pair $(\Lambda_B(K), \Lambda_W(K))$ fails to be a complete mutation invariant:

Theorem. *The pair of lattices of integer flows of the Tait graphs of virtual knots, $(\Lambda_B(V), \Lambda_W(V))$ is not a complete invariant of alternating virtual knots.*

The rest of this text will work up to the proof of this theorem. Chapter 3 introduces the Gordon-Litherland linking form, another mutation invariant of virtual knots whose symmetrisation is equivalent to the lattice of integer flows. Chapter 4 presents algorithms which we use to compute these invariants, to produce the necessary counterexample for the incompleteness theorem.

Chapter 3

Gordon-Litherland Linking Forms

God created the knots. All else in topology is the work of mortals.

— Leopold Kronecker, modified by Dror Bar-Natan

We turn our attention to the work of Cameron Gordon and Richard Litherland, and quietly note that Gordon (1945 – present) may yet disprove this Chapter’s epigraph. This duo assigned a symmetric quadratic form to a knot, based on an unoriented spanning surface of the knot [GL78]. Recent work by Boden-Chrisman-Karmimi extends this to a form in the virtual setting, called the Gordon-Litherland linking form [BCK22]. In this chapter, we define this linking form, prove that it is a mutation invariant of alternating virtual knots, and relate it with the lattice of integer flows of the previous chapter.

Except for the last theorem of this chapter, which is original work, we follow [BCK22; BK23a; BK23b; Bod+15] to describe the Gordon-Litherland form.

3.1 Spanning Surfaces and Linking Numbers

A *spanning surface* of a knot $K \subseteq \Sigma \times I$ is an unoriented surface $S \subset \Sigma \times I$ with boundary $\partial S = K$. The definition of the Gordon-Litherland linking form is based on a choice of spanning surface for the knot.

Recall from Chapter 2 that a knot in a thickened surface is checkerboard colourable if and only if a spanning surface exists. While all classical knots have spanning surfaces, the same is not true in thickened surfaces. From the checkerboard colouring of a knot in $\Sigma \times I$, it is easy to construct a spanning surface. For each coloured region of the surface knot diagram D , we place a corresponding disk in $\Sigma \times \{1/2\}$. For each crossing in D , we place a half-twisted band connecting the two adjacent coloured regions, such that the half-twist in the band agrees with the type of the crossing, as in Fig. 11. We denote this spanning surface F , and the surface obtained by swapping the colourings as F^* . Observe that $F \cup F^* = \Sigma$.

A crucial ingredient in the Gordon-Litherland linking form is the notion of linking numbers. Let J and K be two oriented disjoint simple closed curves in the interior of $\Sigma \times I$. Consider the relative homology group $H_1(\Sigma \times I \setminus J, \Sigma \times \{1\})$. This group is isomorphic to \mathbb{Z} , and generated by a meridian μ of J . The *linking number* of J with K , $\ell k(J, K)$ is defined as the unique integer n such that $[K] = n\mu$. Equivalently, $\ell k(J, K)$ is the signed number of times that J passes above K , with ‘above’ defined to be with respect to t , the parameter of

the interval I . A positive (resp. negative) contribution is made to $\ell k(J, K)$ when J passes over K such that the coordinate system $\hat{j}, \hat{k}, \hat{t}$ has a positive (resp. negative) orientation.

Note that $\ell k(J, K)$ is independent of the number of times that J passes under K : this is instead captured by $\ell k(K, J)$. In general, these two notions are different, except in the classical setting, where linking numbers of curves in $\mathbb{R}^2 \times I$ are symmetric:

$$\ell k(J, K) - \ell k(K, J) = 0.$$

This can be shown by examining the following table of contributions and noticing that when K passes over or under J going ‘up’ (with respect to the page) there is a positive contribution to $\ell k(J, K) - \ell k(K, J)$, and likewise a negative contribution when K passes over or under J going ‘down’.

An application of the Jordan curve theorem implies that the crossings come in cancelling pairs.

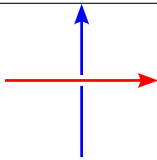
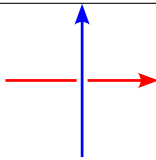
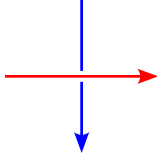
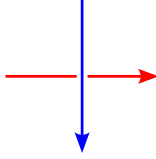
Crossing	$\ell k(J, K)$	$-\ell k(K, J)$	Crossing	$\ell k(J, K)$	$-\ell k(K, J)$
	+1	0		0	+1
	-1	0		0	-1

Table 1: Crossings between J (red) and K (blue) and their contribution to $\ell k(J, K) - \ell k(K, J)$.

A related notion is the intersection pairing on the first homology $H_1(\Sigma)$. The *algebraic intersection number* of two homology classes α and β is the number of times any two representatives of those classes α and β intersect, counted with sign (specifically, the sign of the coordinate system \hat{a}, \hat{b} where a and b are two 1-chains). This is well-defined, as if a and a' are such that $[a] = [a']$, then $[a - a'] = 0$, so there is a 2-chain A such that $\partial A = a - a'$. The intersection number of a closed curve with any 2-chain is 0, so $A \cdot b = 0$, hence $(a - a') \cdot b = 0$, and finally $a \cdot b = a' \cdot b$.

In general in $\Sigma \times I$, linking numbers are not symmetric. Rather, they satisfy the following relationship:

$$\ell k(J, K) - \ell k(K, J) = p_*(J) \cdot p_*(K),$$

where $p : \Sigma \times I \rightarrow \Sigma$ is the projection map which induces $p_* : H_1(\Sigma \times I) \rightarrow H_1(\Sigma)$, and the product \cdot denotes algebraic intersection number. The proof of this fact is an easy modification of the argument above.

3.2 The Linking Form

Consider a (not necessarily orientable) spanning surface F for a knot K . The normal bundle $N(F)$ is a 0, 1-bundle of F . Let ∂F denote the boundary of $N(F)$, this is an orientable double

cover of F . Let $\pi : \tilde{F} \rightarrow F$ denote the covering map. If F was orientable, then this is the trivial 2-sheeted double cover (and hence orientable), and if F was non-orientable, then this is the unique orientable double cover of F . Either way, \tilde{F} is orientable, and by definition oriented.

The *pushoff* of a closed loop γ in F is $\pi^{-1}(\gamma)$. If F was orientable, this is a union of two closed curves, one above γ and one below, whereas if F was non-orientable, this is a single closed curve that passes both above and below γ . We define the *transfer map* $\tau : H_1(F) \rightarrow H_1(\tilde{F})$ by setting $\tau([a]) = [\pi^{-1}(a)]$. Locally, we can also define t^+ and t^- as the two maps $t^\pm : F \rightarrow \tilde{F}$. This way, locally composing a curve γ with t^+ or t^- produces a lift of γ . We define $t(\gamma) = t^+(\gamma) \cup t^-(\gamma)$.

The *Gordon-Litherland linking form* (which we shorten to the *linking form*) on a compact, unoriented spanning surface F of a knot in $\Sigma \times I$ is the bilinear form

$$\mathcal{L}_F : H_1(F) \times H_1(F) \rightarrow \mathbb{Z}$$

defined by

$$\mathcal{L}_F(\alpha, \beta) = \ell k(\tau\alpha, \beta)$$

for $\alpha, \beta \in H_1(F)$. By basic algebraic topology, this does not depend on the choice of representatives [BK23a, Chapter 2].

Given a choice of basis for $H_1(X)$, a pairing matrix for this form is called a *mock Seifert matrix* if its ij entry is $\ell k(\tau\alpha_i, \alpha_j)$ for some basis $\{\alpha_1, \dots, \alpha_n\}$ of $H_1(F)$. The word *mock* here refers to the fact that unlike a classical Seifert matrix, the surface F is not a necessarily orientable; an orientable spanning surface would be called a Seifert surface. As any other unimodular congruent matrix represents the same form \mathcal{L}_F with respect to a different basis, and conversely any change of basis induces a unimodular congruence in the corresponding mock Seifert matrices.

We wait until Chapter 4 to give examples of computations of this form, as that will be the primary focus of the chapter.

As observed in [BCK22, Section 3], the linking forms corresponding to the black and white checkerboard surfaces define an invariant of checkerboard colourable virtual knots, using a minimal genus representative of the knot. Reduced, cellularly embedded alternating diagrams of alternating knots are always minimal genus, hence we have the following special case:

Theorem. *Let V be an alternating virtual knot, and let D and E be reduced, alternating cellularly embedded diagrams of V . Let F_D and F_E (resp. F_D^* and F_E^*) be positive definite (resp. negative definite) spanning surfaces for D and E . Then $\mathcal{L}_{F(D)} \cong \mathcal{L}_{F(E)}$ and $\mathcal{L}_{F_D^*} \cong \mathcal{L}_{F_E^*}$.*

Proof. By Greene's characterisation, F_D and F_E are positive definite surfaces. Kindred [Kin22, Theorem 2.8] shows that Boden-Karimi's proof of Theorem 4.8 in [BK23a] yields the stronger result that both F_D and F_E are isotopic. Hence we have $\mathcal{L}_{F_D} \cong \mathcal{L}_{F_E}$ and $\mathcal{L}_{F_D^*} \cong \mathcal{L}_{F_E^*}$ \square

3.3 The Gordon-Litherland Pairing

The *Gordon-Litherland pairing* is the symmetrisation of the linking form. Namely, given a compact, unoriented spanning surface F of a knot in $\Sigma \times I$ is the symmetric bilinear form

$$\mathcal{G}_F : H_1(F) \times H_1(F) \longrightarrow \mathbb{Z},$$

$$\mathcal{G}_F(\alpha, \beta) = \frac{1}{2}(\ell k(\tau\alpha, \beta) + \ell k(\tau\beta, \alpha)).$$

If a mock Seifert matrix A represents \mathcal{L}_F with respect to some basis of $H_1(F)$, then its symmetrisation $\frac{1}{2}(A + A^T)$ represents the pairing \mathcal{G}_F with respect to the same basis. We say that F is a *positive* (resp. *negative*) *definite surface* if the form \mathcal{G}_F is positive (resp. negative) definite.

Gordon-Litherland [GL78] use the Gordon-Litherland pairing to define a set of link invariants based on this form, including the signature, determinant and nullity of a link. Boden-Chrisman-Karimi [BCK22] define and study the analogous invariants for virtual knots using the virtual Gordon-Litherland pairing.

From the fact that the linking forms \mathcal{L}_F and \mathcal{L}_{F^*} are mutation invariants of alternating knots, it follows that the pairings are as well. In fact, we show the Gordon-Litherland pairing is exactly the lattice of integer flows of the Tait graph of a knot:

Theorem. *Let K be an alternating virtual knot. The Gordon-Litherland pairing on the black surface is equal to the lattice of integer flows of the Tait graph corresponding to the black surface: $\mathcal{G}_F(K) \cong \Lambda_B(K)$. On the other hand, $\mathcal{G}_{F^*}(K) \cong -\Lambda_W(K)$.*

Proof. First note that the black spanning surface F deformation-retracts to the Tait graph corresponding to the black region, G_B , so $H_1(F) \cong H_1(G_B)$. We need to prove that the pairing is the same.

Let α, β be basis elements of $H_1(F)$, and choose representative curves a and b for α and β respectively. The curves can be deformed by homotopy such that when projected onto Σ , they only touch at crossings, so we only need to look at the local contribution at the crossings:

$$\frac{1}{2}(\ell k(ta, b) + \ell k(tb, a)).$$

We show that the local contribution at a crossing is 1 if a and b pass through the crossing in the same direction. By symmetry, the order of the curves doesn't matter, so there are two cases to examine: where the curves intersect tangentially in the projection, and where they intersect transversely. The tangential case is shown in Fig. 25 and explained in the caption. The transverse case is similar. Finally, if α and β don't both pass through a crossing, then the local contribution from that crossing is clearly 0.

By linearity, when the curves pass through the crossing in opposite directions, the local contribution to $\mathcal{G}_F(\alpha, \beta)$ is -1 .

Via the identification $H_1(F) \cong H_1(G_B)$, the curves correspond to cycles in the Tait graph, whose edges are identified with the crossings. Therefore, \mathcal{G}_F counts with sign, the common edges between cycles of G_B . This is by definition the inner product on the lattice of integer flows of G_B .

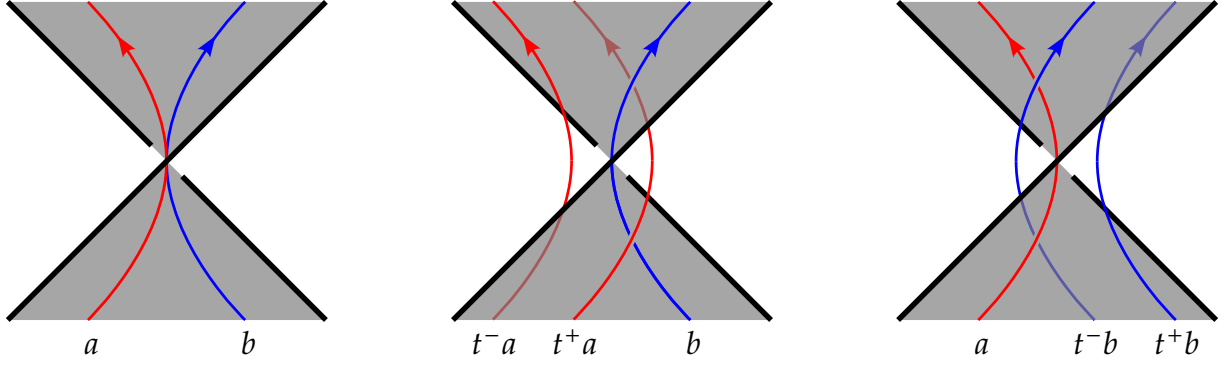


Figure 25: A local contribution to $\mathcal{G}_F(\alpha, \beta)$ from the curves a and b . The left shows the initial geometry of a and b . The middle and right images illustrate that $\ell k(ta, b) = 1$ and $\ell k(tb, a) = 1$.

The same argument applies for the white checkerboard surface, but since the crossings are now of opposite type, we get opposite sign local contributions to $\mathcal{G}_{F^*}(\alpha, \beta)$ in each case. Hence, $\mathcal{G}_{F^*}(K) \cong -\Lambda_W(K)$. \square

We obtain as a corollary the theorem we left unproven in Chapter 2:

Corollary. *Let V be an alternating virtual knot, and let D, E be alternating surface knot diagrams for V . Then $\Lambda_B(D) \cong \Lambda_B(E)$ and $\Lambda_B(D) \cong \Lambda_W(E)$.*

It also follows that the Gordon-Litherland pairing is a mutation invariant.

Corollary. *Let D and E be two surface knot diagrams, possibly for different knots, related by a sequence of disk mutations. Then $\mathcal{G}_{F_D} \cong \mathcal{G}_{F_E}$ and $\mathcal{G}_{F_D^*} \cong \mathcal{G}_{F_E^*}$.*

Proof. In Chapter 1, we saw that mutation either merely changes the embedding of the Tait graph in the plane, or induces a Whitney flip in the Tait graph. The same argument proves that a disk mutation either changes the embedding of the Tait graph in Σ , or induces a Whitney flip. The lattice of integer flows is independent of the embedding and invariant under Whitney flips, completing the proof. \square

In fact, \mathcal{L}_F is also a mutation invariant, which we will prove in Chapter 4 using a formula in terms of \mathcal{G}_F and the intersection pairing.

Chapter 4

Computing Mock Seifert Matrices

In these days the angel of topology and the devil of abstract algebra fight for the soul of each individual mathematical domain.

— Hermann Weyl, *Invariants*

Better to reign in Hell than to serve in Heaven.

— John Milton, *Paradise Lost*

In this chapter, which is my own original work, provide algorithms for computing the ribbon Tait graphs and mock Seifert matrices of virtual knots. The lattice of integer flows of the Tait graph, the d -invariants, and the mock Alexander polynomial are easily computable from the mock Seifert matrices, which I have also implemented. In section 5, I give a counterexample proving that the pair $(\Lambda_B(K), \Lambda_W(K))$ is not a complete mutation invariant of alternating knots.

Results of the algorithms for tabulated virtual alternating knots (up to 6 crossings), as well as a link to a Python implementation of the algorithms are attached in Appendix A.

4.1 Gauss Codes and Gauss Diagrams

Knot diagrams, being geometric objects are difficult for computers to directly handle. However, since knot diagrams are considered up to planar isotopy/surface isotopy, the information contained within them is completely combinatorial. The *Gauss code* of an oriented knot diagram encodes this combinatorial information by recording the order in which the crossings are visited, as the diagram is traversed. In other words, the Gauss code is a sequence of crossings (usually given by labels $\{1, \dots, n\}$), along with a symbol describing whether a crossing is traversed via the over-strand or the under-strand. This is, of course, only unique up to cyclic permutation. For example, the diagram of the figure eight knot in Fig. 26a has Gauss code

1O 2U 3O 4U 2O 1U 4O 3U.

We call a crossing in an oriented knot diagram *positive* if it can be rotated to look like Fig. 27a, and *negative* if it can be rotated to look like Fig. 27b. This is referred to as the *sign* or *writhe* of the crossing.

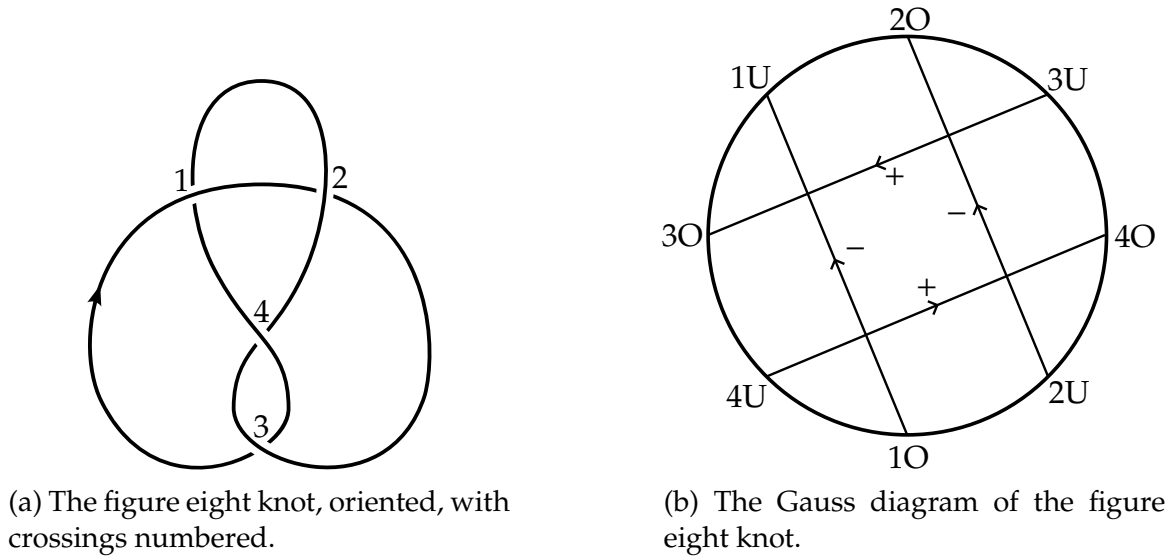


Figure 26: A diagram and its gauss diagram for the knot 4_1 .



Figure 27: Crossing sign or writhe.

The Gauss code can be extended to incorporate the writhe, also known as the sign, of each crossing, and in doing so, each element of the sequence also incorporates a sign of +1 for a positive crossing, or -1 for a negative crossing. The extended Gauss code from Fig. 26a, is

$$-1O - 2U + 4O + 3U - 2O - 1U + 3O + 4U.$$

since crossings 1 and 2 are negative, and crossings 3 and 4 are positive. Henceforth we refer to the extended Gauss Code as simply the Gauss code.

The Gauss code extends naturally to virtual knots, as it takes into account only combinatorial information about the crossings, and it is oblivious to the diagram's planarity (or lack thereof). In the Gauss code of a virtual knot, virtual crossings make no contribution.

In fact, modulo cyclic permutation of the code, the set of Gauss codes exactly corresponds to the set of virtual knot diagrams. This gives another completely combinatorial definition of virtual knots as equivalence classes of Gauss codes, modulo cyclic permutation and Gauss code Reidemeister moves.

The *Gauss diagram* of a knot diagram consists of a cyclic ordering of the $2n$ words of the Gauss code around the circle, with n directed edges (chords) from the word iO to the word

iU for each $i \in \{0, \dots, n\}$. These chords represent crossings, and are labelled according to the crossing's sign. Arcs of the Gauss diagram between words represent arcs on the knot diagram between crossings.

4.2 Reconstructing the Ribbon Tait Graph

Recall that a virtual knot has a Tait graph if and only if it is checkerboard colourable. For these knots, Gauss code uniquely determines the Tait graph, in fact, the ribbon Tait graph. In this section we provide an algorithm for explicitly reconstructing the ribbon Tait graph from Gauss code.

The idea of the algorithm is as follows. Vertices in the Tait graph, correspond to faces in the knot diagram, and edges in the Tait graph correspond to crossings in the diagram. To walk around a given face of the knot diagram, we traverse along the strands, and each time we encounter a crossing, we 'hop' to the other strand at that crossing to continue our traversal.

There is a choice regarding which direction to traverse the new strand, and to keep circling, we need to always turn in the same direction (always left or always right). We have no a priori notion of 'left' or 'right' in the Gauss code, but we can ensure that we choose the correct turn direction by appropriately choosing whether to continue traversing with or against the orientation after each 'hop'. To make this decision, we need information about the sign of the crossing and whether the hop was from an over-strand to an under-strand or vice-versa.

Knowing how to traverse a face, we traverse all faces corresponding to the black checkerboard colouring. In doing so, we keep track of which crossings we encountered when traversing each face, and the order in which we encountered them. When the algorithm terminates, each crossing is associated with two faces. This defines a graph with faces as vertices and an edge for each crossing between the two associated faces – the Tait graph.

This can be done completely combinatorially from the Gauss Code, but we present it here as a graph algorithm on the Gauss diagram. By an *arc*, we mean a path in the knot diagram between two adjacent crossings (with no intermediate crossings in the traversal).

Algorithm

Throughout let n be the crossing number of the diagram D .

#	Step	Explanation/Notes
1.	For each $i \in \{1, \dots, n\}$, initialise a two-element array F_i .	The list F_i will keep track of which two checkerboard coloured faces are incident to each vertex.
2.	Initialise a counter $f = 1$.	This algorithm iterates over the faces in the knot diagram, so we maintain a counter, f , of the face presently being examined.

3. Initialise variable $t = 1$.

As we traverse each face, we must maintain a constant turning direction to pick out faces of the knot diagram. We use the convention

$$t = \begin{cases} -1 & \text{for left turn,} \\ +1 & \text{for right turn,} \end{cases}$$

and we ensure that this variable is constant over each face.

4. Until we have visited every chord, do the following loop:

We loop over the faces.

- 4.1. Initialise variable $a = 1$.

Since we do not have the knot diagram, we cannot choose to turn left or right directly. Instead, when we 'hop' strands, we will have to choose to align or anti-align with the orientation of the new strand. We keep track of this with the convention:

$$a = \begin{cases} -1 & \text{if aligned with orientation,} \\ +1 & \text{if anti-aligned with orientation,} \end{cases}$$

and whenever we hop strands we will update a in a way that ensures we always turn left or right.

- 4.2. Initialise a list R_f .

The arrays R_f keep track of the cyclic order that crossings were visited around face f , which translates into the cyclic order of edges around each vertex of the Tait graph.

- 4.2. Until we reach the same chord and have $a = 1$, perform the following loop:

- 4.2.1 Traverse an arc of the Gauss diagram anti-clockwise if $a = 1$, clockwise if $a = -1$.

This corresponds to travelling from the current over-/under-crossing to the next crossing along a strand of the diagram, with or against the orientation depending on the value of a .

4.2.2 Traverse the chord of the Gauss diagram at the current word. Append f to the list F_i and append i to R_f where i is the crossing number that the chord corresponds to.

This corresponds to the ‘hop’ between under- and over-strands at a crossing.

4.2.3 Update the value of a :

$$a \leftarrow t \cdot j \cdot w \cdot a$$

This ensures that we are consistently turning left (or consistently turning right) within a face, see Step 4.1.

where w is the writhe (sign) of the current crossing and j is $+1$ or -1 based on the ‘hop’ we completed in the previous step.

We use the convention

$$j = \begin{cases} -1 & \text{for hops over} \rightarrow \text{under,} \\ +1 & \text{for hops under} \rightarrow \text{over.} \end{cases}$$

4.3 Continue the loop in Step 4.2, or move on if the condition is satisfied.

4.4 If $t = -1$, reverse the cyclic ordering in R_f .

This ensures that all R_f are oriented the same way with respect to the underlying orientable surface.

4.5 Continue the loop in Step 4. Start at the next chord yet to be traversed (in anti-clockwise order around the Gauss diagram), and update t :

Repeat loop for next face, or move on if there are no more faces. The update rule ensures that we are only visiting faces in the black (or white) checkerboard colouring.

$$t = (-1)^k$$

where k is the index of this chord around the chord diagram, with counting starting from 0.

5. Once all chords have been traversed, construct the graph G with vertex list $\{1, \dots, n\}$ and an edge between each pair of vertices in some F_i , $i \in \{1, \dots, n\}$. The set $\{R_v \mid v \in \{1, \dots, n\}\}$ is a rotation system for G .

To illustrate the algorithm, we give an example reconstruction of the Tait graph of the diagram of virtual knot 4_{106} seen in Fig. 28a with Gauss code

$$-1\text{O} - 2\text{U} - 3\text{O} - 1\text{U} + 4\text{O} - 3\text{U} - 2\text{O} + 4\text{U}.$$

We have provided the knot diagram for illustrative purposes only, and it is important to

note that the diagram is not necessary for the algorithm. The traversal paths in the graph algorithm are shown in Fig. 29.

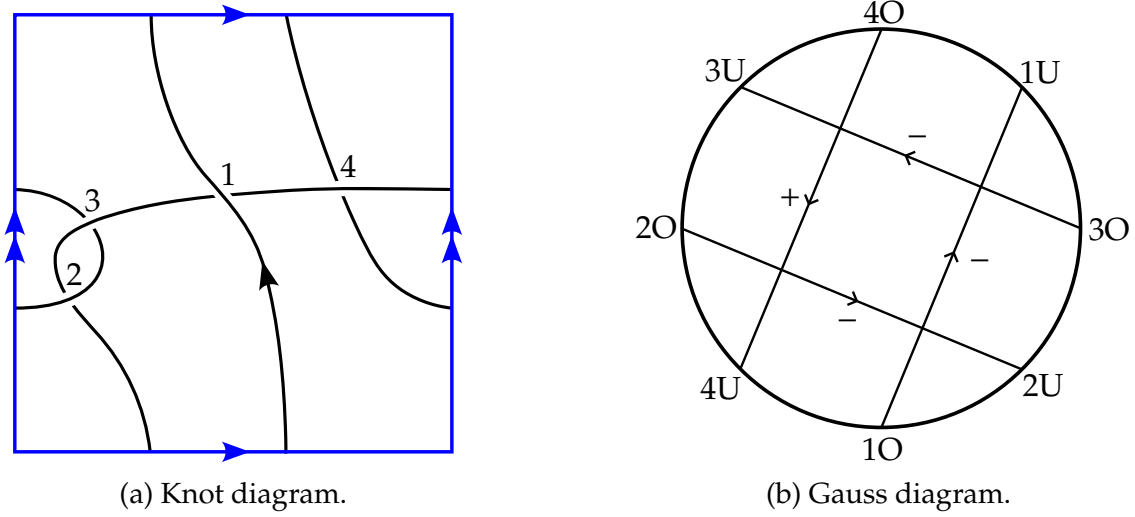


Figure 28: A knot diagram of 4_{106} and its Gauss diagram.

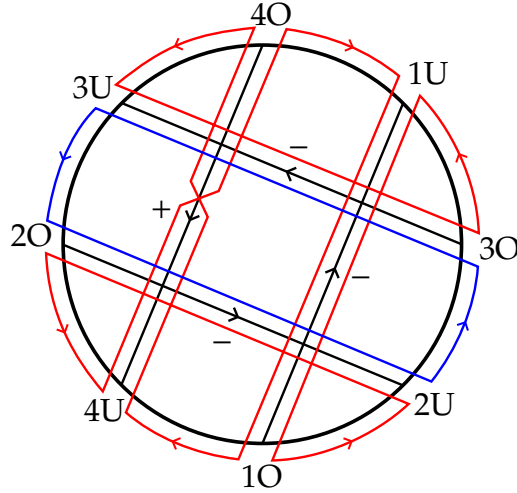


Figure 29: The Gauss diagram of the diagram of 4_{106} in Fig. 28a with the traversal paths shown for $f = 1$ (red) and $f = 2$ (blue).

When the algorithm terminates, the ribbon Tait graph is given by vertex set $V = \{1, 2\}$, corresponding to the red and blue loops in Fig. 29, with four edges: e_1 and e_2 connecting v_1 and v_2 , and two e_3 and e_4 connecting v_1 to itself. We obtain the rotation system $R_1 = [e_2, e_4, e_1, e_4, e_3, e_1]$, $R_2 = [e_2, e_3]$ from which we can see that this Tait graph is not planar. This is indeed the same ribbon Tait graph as the one obtained from the knot diagram in Fig. 28a.

To find the white Tait graph, we use the same algorithm, but with the opposite initial turn direction ($t = -1$), and opposite (negative) update rule in Step 4.5.

Proposition. *The algorithm given above finds the Tait graphs from the Gauss code of a virtual knot.*

Proof. If the algorithm traverses the black (resp. white) coloured regions of the checkerboard coloured knot diagram turning in a consistent direction at each face, and it eventually traverses every coloured face, then it produces the black (resp. white) Tait graph.

The first claim is that the update rule

$$a \leftarrow t \cdot j \cdot w \cdot a$$

turns consistently left when $t = 1$ or right when $t = -1$. We show four cases of this in Fig. 30, namely the cases $t = 1, j = \pm 1, w = 1, a = \pm 1$. For example in the case that we are traversing the knot diagram into this crossing from the top-left of the crossing, we have $t = 1, j = -1, w = 1, a = -1$. Hence we update a to $t \cdot j \cdot w \cdot a = 1$, and therefore hop to the over-strand and continue traversing with the alignment of the over-strand. In fact, it suffices to check this one case, and generate the other 15 by the symmetries $t \mapsto -t, j \mapsto -j, w \mapsto -w, a \mapsto -a$.

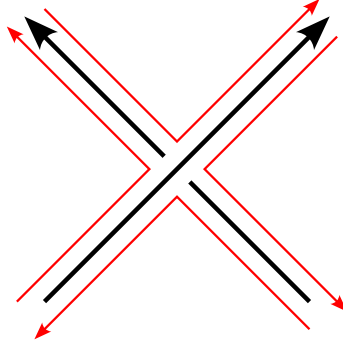


Figure 30: Some cases of the alignment update rule.

The second claim is that the update rule $t = (-1)^k$ picks out black checkerboard coloured faces. Consider the regular traversal (without jumping at crossings) of the checkerboard coloured knot diagram. Initially, the checkerboard coloured region is on our left, but after the first crossing it swaps to be on the right, and continues swapping at each crossing we encounter. Hence after the k th crossing, we choose $t = (-1)^k$, and so the algorithm traverses only black faces until there are none left. \square

4.3 Mock Seifert Matrices: Preliminaries

As the Tait graphs $G_B(D)$ and $G_W(D)$ along with their rotation systems determine an surface embedding of each of these graphs, it is possible to compute mock Seifert matrices corresponding to $\mathcal{G}_F(K)$ and $\mathcal{G}_{F^*}(K)$.

Proposition. *The algebraic intersection numbers of the projections of curves into Σ is expressible in terms of the linking number of the curves,*

$$p_*(\alpha) \cdot p_*(\beta) = \frac{1}{2} (\ell k(\tau\alpha, \beta) - \ell k(\tau\beta, \alpha))$$

Proof. We proceed similarly to the proof in Section 3.3, by letting α and β be basis elements for $H_1(F)$, choosing representative curves a and b so that in the projection the only intersect at crossings. Then we examine the local contribution to $p_*(\alpha) \cdot p_*(\beta)$ at each crossing.

There are two cases: curves may intersect in the projection either tangentially or transversely. Fig. 31 showcases the transverse case. We see that locally $\ell k(\tau\alpha, \beta) = 2$ and $\ell k(\tau\beta, \alpha) = 0$, hence $\frac{1}{2}(\ell k(\tau\alpha, \beta) - \ell k(\tau\beta, \alpha)) = 1 = p_*(\alpha) \cdot p_*(\beta)$. The tangential case is similar.

Since both \cdot and ℓk are bilinear, this completes the proof. \square

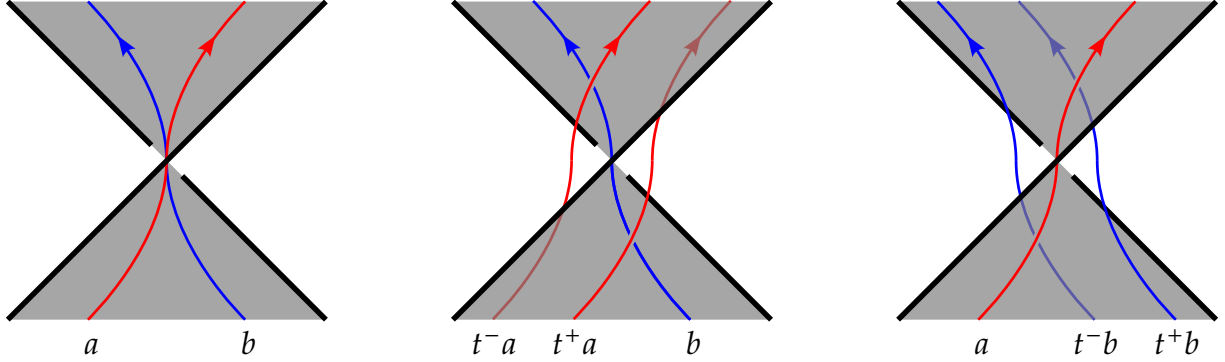


Figure 31: Some cases of the alignment update rule.

This implies the following corollary (which is actually the definition of \mathcal{G}_F in [BCK22]).

Corollary. *The linking form is related to the Gordon-Litherland pairing by*

$$\mathcal{L}_F(\alpha, \beta) = \mathcal{G}_F(\alpha, \beta) + p_*(\alpha) \cdot p_*(\beta)$$

Proof.

$$\begin{aligned} \mathcal{L}_F(\alpha, \beta) &= \ell k(\tau\alpha, \beta) \\ &= \frac{1}{2} \ell k(\tau\alpha, \beta) + \frac{1}{2} \ell k(\tau\alpha, \beta) \\ &= \frac{1}{2} \ell k(\tau\alpha, \beta) + \frac{1}{2}(\tau\beta, \alpha) + \frac{1}{2} \ell k(\tau\alpha, \beta) - \frac{1}{2}(\tau\beta, \alpha) \\ &= \mathcal{G}_F(\alpha, \beta) + p_*(\alpha) \cdot p_*(\beta). \end{aligned}$$

\square

This gives us a way to compute the linking form of a given spanning surface: we simply compute the lattice of integer flows of the corresponding Tait graph, which is easy, then add the intersection numbers of the curve projections, which is more involved.

The following proposition of Boden-Karimi [BK23b, Remark 3.2] simplifies this computation.

Proposition. *Let $i : F \longrightarrow \Sigma \times I$ be the inclusion map. The restriction of \mathcal{L}_F to the kernel of $i_* : H_1(F) \longrightarrow H_1(\Sigma \times I)$ is symmetric. In fact, if $\alpha \in \ker i_*$ or $\beta \in \ker i_*$, then $\mathcal{L}_F(\alpha, \beta) = \mathcal{L}_F(\beta, \alpha)$.*

Proof. Let a, b be representative curves for α, β . Without loss of generality assume $\alpha \in \ker i_*$. Then a is null-homotopic in $\Sigma \times I$, so $p(a)$ is null-homotopic in Σ . Applying the Jordan Curve Theorem on Σ shows that $p_*(\alpha) \cdot p_*(\beta) = 0$. The formula above and the fact that $\mathcal{G}_F(\alpha, \beta)$ is symmetric completes the proof. \square

We obtain as a corollary that \mathcal{L}_F is a mutation invariant.

Corollary. *Let D and E be two surface knot diagrams, possibly for different knots, related by a sequence of disk mutations. Then $\mathcal{L}_{F_D} \cong \mathcal{L}_{F_E}$ and $\mathcal{L}_{F_D^*} \cong \mathcal{L}_{F_E^*}$.*

Proof. We prove this for a single mutation and the result follows by induction.

Since

$$\mathcal{L}_F(\alpha, \beta) = \mathcal{G}_F(\alpha, \beta) + p_*(\alpha) \cdot p_*(\beta),$$

and we showed at the end of Chapter 2 that \mathcal{G}_F is mutation invariant, it suffices to prove that the algebraic intersection number $p_*(\alpha) \cdot p_*(\beta)$ is a mutation invariant.

If $i_*(\alpha) = 0$ or $i_*(\beta) = 0$, then $p_*(\alpha) \cdot p_*(\beta) = 0$ both before and after mutation. Hence it is only required to check invariance for a set of cycles whose inclusions into Σ form a basis for $H_1(\Sigma)$.

The mutation disc B intersects $D = \partial F$ at four points. If the two connected components of $(\partial B) \cap p(F)$ are not connected by a path in $B \cap p(F)$, then we may always choose representative curves that are disjoint from B , so mutation does not affect the intersection pairing.

If the two connected components of $(\partial B) \cap p(F)$ are connected by a path in $B \cap p(F)$, we show that the set of representatives can be chosen so that at most one of them intersects B . For contradiction, assume that there are two representatives α and β , both of which pass through B . We may assume that both α and β enter via one component of $\partial B \cap p(F)$ and exit through the other (otherwise their intersection with B can be eliminated). Assume α and β both enter and exit D once, and in the same direction. Then replace β among the representatives with $\beta' = \beta - \alpha$. This new set of representatives still surjects onto $H_1(\Sigma)$, and there is a curve homologous to β' which does not pass through B . The cases of opposite directions and multiple entries are dealt with similarly.

Since only one of the representatives passes through B , mutation does not affect the intersection pairing. This completes the proof. \square

Another corollary of this proposition is that there is a particularly nice way to present mock Seifert matrices. If we choose a basis for $H_1(X)$ of the form $\{\gamma_1, \dots, \gamma_k, \gamma_{k+1}, \dots, \gamma_n\}$ where $\{\gamma_1, \dots, \gamma_k\}$ forms a basis for $\ker i_*$, then the resulting mock Seifert matrix M will be of block form

$$M = \begin{bmatrix} A & B^\top \\ B & S \end{bmatrix}$$

where A is an asymmetric $k \times k$ matrix, B is a $k \times (n - k)$ matrix and S is a symmetric $(n - k) \times (n - k)$ matrix.

Having mock Seifert matrices in this form, it is also easier, in special cases, to detect unimodular congruences, which is a complicated problem.

4.4 Computing Mock Seifert Matrices

We now present the algorithm for computing a mock Seifert matrix of a knot diagram. We first compute a basis so that the mock Seifert matrix is as in the proposition above. The idea of the algorithm is as follows.

Choose representative curves as cycles in the Tait graph for basis elements of the first homology $H_1(F)$. In this way, we can compute the lattice of integer flows easily as discussed in Chapter 3.

To compute the algebraic intersection form, it suffices to compute local contributions at each vertex of the Tait graph. Consider the information about the Tait graph available locally at each vertex: there are several edges with a cyclic ordering from the rotation system, and for each pair α and β in the basis for $H_1(F)$, some of these edges have non-zero coefficients in the cycle α (resp. β). If this is the case, we say an edge belongs to α (resp. β).

If the edges that belong to α are distinct from the edges that belong to β , the algebraic intersection number $p_*(\alpha) \cdot p_*(\beta)$ is easy to compute. We call it a *degeneracy* when the edges that belong to α and the edges that belong to β have non-empty intersection, say at edge e . In this case, there is not locally enough information to know whether at edge e , whether α or β should come first when computing the algebraic intersection number: this information is too far away to be seen by the vertex.

For example, on the graph in Fig. 32a, consider $\alpha = [e_1 + e_8 + e_7 + e_2]$ and $\beta = [e_3 + e_2 + e_4 + e_5 + e_6]$. At v_1 , there is no degeneracy, and the local contribution to the algebraic intersection number $p_*(\alpha) \cdot p_*(\beta) = 1$. However at v_2 , there is a degeneracy along e_2 .

We say we resolve a degeneracy *prioritising* α (resp. β) if relative to the cyclic order, we put α (resp. β) first. Fig. 32b (resp. Fig. 32c) shows this. Note the differences in local contributions.

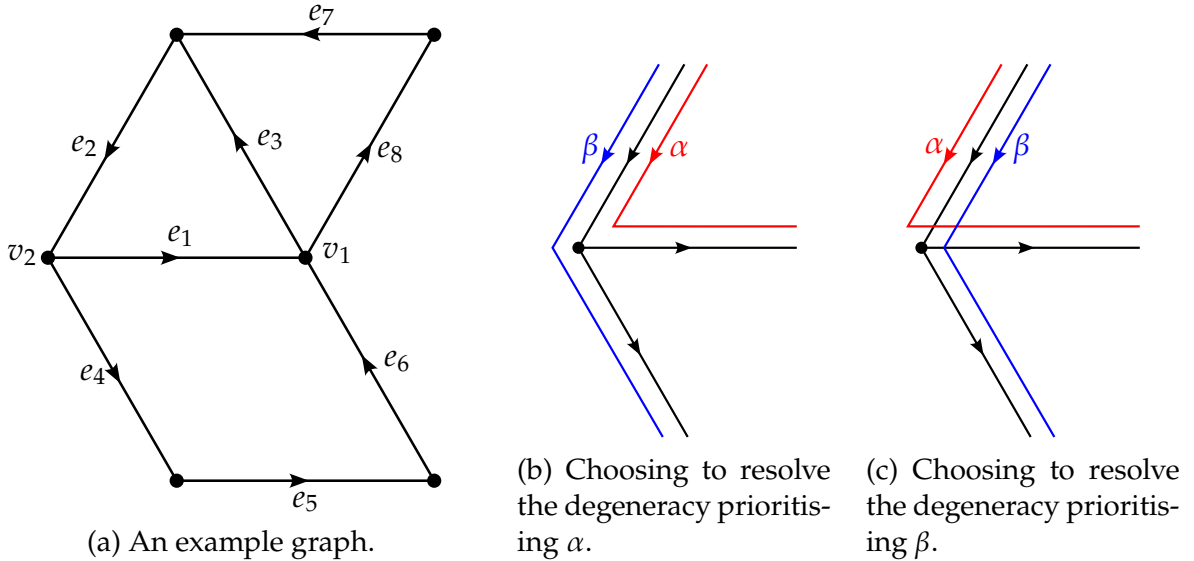


Figure 32: An example of a degeneracy between α (red) and β (blue) and the two ways to resolve it. In (b) there is a local contribution of 0, while in (c) there is a local contribution of -1 .

The key observation for the algorithm is that by resolving degeneracies both ways at every vertex and averaging the local contributions give the correct total contribution.

Algorithm

#	Step	Explanation/Notes
1.	Compute a basis for $\ker i_* : H_1(F) \rightarrow H_1(\Sigma \times I)$.	A face in $G_B(D)$ can be written as a cycle of edges $G_W(D)$. The rotation system R_f of $G_B(D)$ contains this information. There are technical implementation details involved here. An implementation can be found in Appendix A.
2.	Extend the basis of $\ker i_*$ to a basis of $H_1(F) \cong H_1(G_B)$.	We choose a basis of $H_1(F)$ to be ordered as a basis for $(\ker i_*)^\perp$, then a basis for $\ker i_*$.
3.	Compute the pairing matrix for $\Lambda_B(G) \cong \mathcal{G}_F$ with respect to this basis.	If A is the basis matrix in which each basis element is a column vector of edges of G_B , then this is $A^\top A$.
4.	For each $\alpha, \beta \in \{\gamma_1, \dots, \gamma_k\}$, compute the pairing matrix element $p_*(\alpha) \cdot p_*(\beta)$ of the algebraic intersection form as follows:	
4.1.	While each α and β in the basis, as cycles of edges.	
4.2.	For $\eta \in \{\alpha, \beta\}$, resolve degeneracies by prioritising η . With degeneracies resolved, compute the local contribution to the algebraic intersection number as follows:	Steps 4.2.1 to 4.2.4 algorithmically compute local contributions to intersection numbers.
4.2.1.	Turn the cyclic ordering into a list by picking an initial item.	
4.2.2.	Initialise a variable $S = 0$.	S for sum.
4.2.3.	Initialise a variable $i = 0$.	

- 4.2.4. Iterate through the list, and when encountering a edge belonging to α , increment i by 1 if α is oriented out of v through that edge, and increment i by -1 if α is oriented into v through that edge. When encountering a edge belonging to β , increment S by i if β is oriented out of v through that edge, and $-i$ if β is oriented into v through that edge.
- 4.3. Average the two local contributions computed in Steps 4.2.1 to 4.2.4. If there are no degeneracies, the two contributions will be the same.
5. Add the pairing matrix for \mathcal{G}_F and the pairing matrix for the algebraic intersection form. The result is a mock Seifert matrix for \mathcal{L}_F .

Proposition. *The algorithm given above computes a mock Seifert matrix for F .*

Proof. The fact that \mathcal{G}_F coincides with the lattice of integer flows in was proven in Chapter 3. It remains to check that the algorithm computes algebraic intersection numbers correctly.

That steps 4.2.1 through 4.2.4 correctly compute local contributions once degeneracies are removed is a simple case analysis of the order and orientation of the whiskers at v belonging to α and β .

We claim that the averaging of degeneracies computes the correct local contribution. Note that degeneracies are along edges, and therefore the same degeneracy always shows up at a pair of vertices (on either end of the edge). When averaging over the two degeneracies, the resolutions match up in pairs to form the correct contributions. There are two such contributions, and a half was introduced in the average, so the contributions are correct. \square

4.5 Incompleteness of the Virtual Gordon-Litherland Pairing

The algorithm above leads to a computational method to find a counterexample to the completeness of the invariant $(\Lambda_B(V), \Lambda_W(V))$ as follows.

Compute mock Seifert matrices $(M_B(V), M_W(V))$ and Gordon-Litherland pairing matrices $(S_B(V), S_W(V))$. Suppose the existence of a pair of knots V_1 and V_2 with pairwise unimodular congruent $(S_B(V_i), S_W(V_i))$ but with pairwise distinct (not unimodular congruent) $(M_B(V_i), M_W(V_i))$. Such a pair has equivalent invariants $(\Lambda_B(V_i), \Lambda_W(V_i))$, as this is equivalent to the $(S_B(V_i), S_W(V_i))$. At the same time, V_1 and V_2 have pairwise non-equivalent linking forms $(\mathcal{L}_F(V_i), \mathcal{L}_{F^*}(V_i))$, implying that they are not mutants.

Of the 92800 virtual knots up to 6 crossings, 164 are alternating. A list of these virtual knots was provided by Hans Boden and created by Lindsay White, and is available in Appendix A. For these virtual knots, we computed the above invariants and found

multiple counterexample pairs. The full results of the computation are available via the link in Appendix A. One of the simplest pairs is shown in Fig. 33 and they have Gordon-Litherland pairing matrices

$$\begin{aligned}
S_B(6_{90101}) &= \begin{bmatrix} 2 & 0 & 0 & 0 \\ 0 & 1 & 0 & 0 \\ 0 & 0 & 2 & 0 \\ 0 & 0 & 0 & 1 \end{bmatrix} & S_W(6_{90101}) &= \begin{bmatrix} 1 & 0 & 0 & 0 & 1 & -1 \\ 0 & 1 & 0 & 0 & 0 & 0 \\ 0 & 0 & 1 & 0 & 0 & 1 \\ 0 & 0 & 0 & 1 & 0 & 0 \\ 1 & 0 & 0 & 0 & 2 & -2 \\ -1 & 0 & 1 & 0 & -2 & 4 \end{bmatrix} \\
S_B(6_{90124}) &= \begin{bmatrix} 2 & 0 & 0 & 0 \\ 0 & 1 & 0 & 0 \\ 0 & 0 & 2 & 0 \\ 0 & 0 & 0 & 1 \end{bmatrix} & S_W(6_{90101}) &= \begin{bmatrix} 1 & 0 & 0 & 0 & 1 & -1 \\ 0 & 1 & 0 & 0 & 0 & 0 \\ 0 & 0 & 1 & 0 & 0 & 1 \\ 0 & 0 & 0 & 1 & 0 & 0 \\ 1 & 0 & 0 & 0 & 2 & -2 \\ -1 & 0 & 1 & 0 & -2 & 4 \end{bmatrix},
\end{aligned}$$

and the mock Seifert matrices

$$\begin{aligned}
M_B(6_{90101}) &= \begin{bmatrix} 2 & -1 & 0 & 0 \\ 1 & 1 & 0 & 0 \\ 0 & 0 & 2 & -1 \\ 0 & 0 & 1 & 1 \end{bmatrix} & M_W(6_{90101}) &= \begin{bmatrix} 1 & 1 & 0 & 0 & 1 & -1 \\ -1 & 1 & 0 & 0 & 0 & 0 \\ 0 & 0 & 1 & 1 & 0 & 1 \\ 0 & 0 & -1 & 1 & 0 & 0 \\ 1 & 0 & 0 & 0 & 2 & -2 \\ -1 & 0 & 1 & 0 & -2 & 4 \end{bmatrix} \\
M_B(6_{90124}) &= \begin{bmatrix} 2 & -1 & 0 & -1 \\ 1 & 1 & 0 & 1 \\ 0 & 0 & 2 & -1 \\ 1 & -1 & 1 & 1 \end{bmatrix} & M_W(6_{90124}) &= \begin{bmatrix} 1 & 1 & -1 & 0 & 1 & -1 \\ -1 & 1 & 1 & 0 & 0 & 0 \\ 1 & -1 & 1 & 1 & 0 & 1 \\ 0 & 0 & -1 & 1 & 0 & 0 \\ 1 & 0 & 0 & 0 & 2 & -2 \\ -1 & 0 & 1 & 0 & -2 & 4 \end{bmatrix}.
\end{aligned}$$

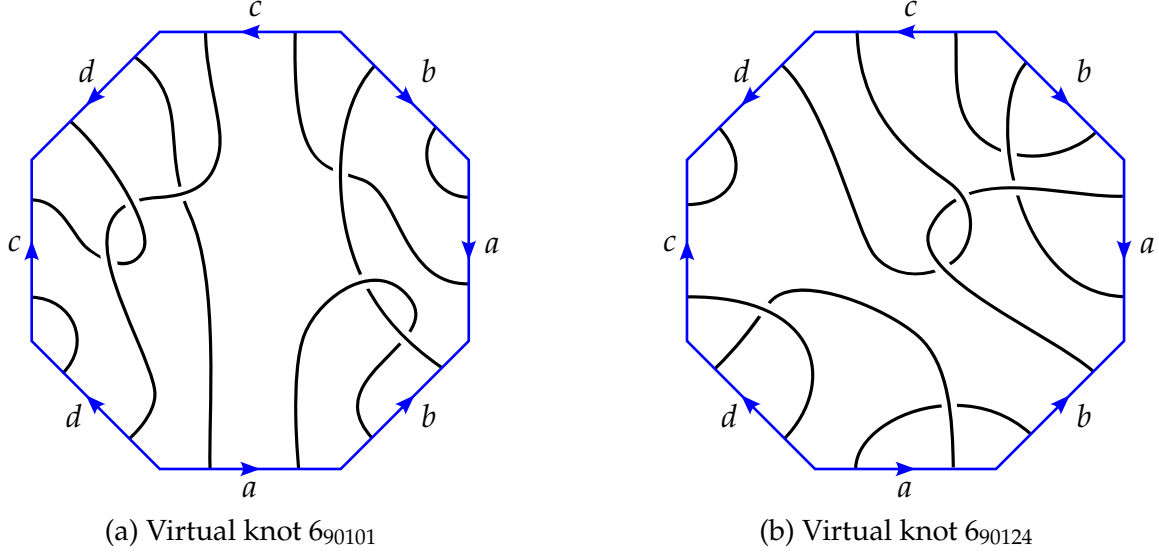


Figure 33: A pair of genus 2 virtual knots providing a counterexample to the completeness of $(\Lambda_B(V), \Lambda_W(V))$.

The pair's Gordon-Litherland pairing matrices are unimodular congruent, by virtue of being identical. To prove that $M_B(6_{90101})$ and $M_B(6_{90124})$ are not unimodular congruent, we look at invariants of unimodular congruence.

Proposition. *The determinant, $\det A$, the Kobayashi invariant, $\text{kob } A := \text{tr}(A^\top A^{-1})$ [SK19] and the matrix Alexander polynomial $\Delta_A(t) := \det(tA - A^\top)$ [BK23b] are invariants of unimodular congruence.*

The implementation in Appendix A also computed these invariants of all matrices. We have

$$\begin{aligned}\det M_B(6_{90101}) &= 9 \\ \det M_B(6_{90124}) &= 15\end{aligned}$$

and

$$\begin{aligned}\det M_W(6_{90101}) &= 9 \\ \det M_W(6_{90124}) &= 15.\end{aligned}$$

This completes the proof of the following corollary.

Corollary. *The pair of lattices of integer flows of the Tait graphs of virtual knots, $(\Lambda_B(V), \Lambda_W(V))$ is not a complete invariant of alternating virtual knots.*

4.6 A Note on Invariants of Unimodular Congruence

From the tables I produced, I noticed that the Kobayashi invariant [SK19], defined as

$$\text{kob } A = \text{tr}(A^\top A^{-1})$$

always satisfied a relation involving the coefficients of the matrix Alexander polynomial [BK23b]

$$\Delta_A(t) := \det(tA - A^\top).$$

Proposition. *The Kobayashi invariant satisfies*

$$\text{kob } A = -\frac{a_1}{a_0}$$

where a_i is the i th coefficient of the Alexander polynomial $\Delta_A(t)$.

Proof. The matrix A , being a mock Seifert matrix, has odd determinant [BK23b] and is therefore invertible. Hence by the multiplicity of determinants,

$$\det(tA - A^\top) = \det(A) \det(tI - A^\top A^{-1}).$$

The last factor here is the characteristic polynomial of $A^\top A^{-1}$. It is a well known fact that the zeroth and first coefficients of the characteristic polynomial of M , are $\det(M)$ and $-\text{tr}(M)$ respectively. Hence,

$$-\frac{a_1}{a_0} = \frac{\text{tr}(A^\top A^{-1})}{\det(A^\top A^{-1})}.$$

Since $\det(A^\top A^{-1}) = \det(A^\top) \det(A^{-1}) = \det(A) \det(A^{-1}) = 1$, we have

$$-\frac{a_1}{a_0} = \text{tr}(A^\top A^{-1})$$

as required. □

This means in particular that the Kobayashi invariant is weaker than the Alexander polynomial.

References

- [AB26] J. W. Alexander and G. B. Briggs. “On Types of Knotted Curves”. In: *Annals of Mathematics* 28.1/4 (1926), pp. 562–586. ISSN: 0003486X. URL: <http://www.jstor.org/stable/1968399> (visited on 04/03/2023).
- [Ada94] C.C. Adams. *The Knot Book*. W.H. Freeman, 1994. ISBN: 9780821886137. URL: https://www.math.cuhk.edu.hk/course_builder/1920/math4900e/Adams--The%20Knot%20Book.pdf.
- [BCK22] Hans U. Boden, Micah Chrisman, and Homayun Karimi. “The Gordon–Litherland pairing for links in thickened surfaces”. In: *International Journal of Mathematics* 33.10n11 (2022). DOI: [10.1142/S0129167X22500781](https://doi.org/10.1142/S0129167X22500781). eprint: <https://doi.org/10.1142/S0129167X22500781>. URL: <https://doi.org/10.1142/S0129167X22500781>.
- [BD16] Dror Bar-Natan and Zsuzsanna Dancso. “Finite-type invariants of w-knotted objects, I: w-knots and the Alexander polynomial”. In: *Algebraic Geometry & Topology* 16.2 (2016), pp. 1063–1133. DOI: [10.2140/agt.2016.16.1063](https://doi.org/10.2140/agt.2016.16.1063). URL: <https://doi.org/10.2140/agt.2016.16.1063>.
- [BD17] Dror Bar-Natan and Zsuzsanna Dancso. “Finite type invariants of w-knotted objects II: tangles, foams and the Kashiwara–Vergne problem”. In: *Mathematische Annalen* 367.3 (Apr. 2017), pp. 1517–1586. ISSN: 1432-1807. DOI: [10.1007/s00208-016-1388-z](https://doi.org/10.1007/s00208-016-1388-z). URL: <https://doi.org/10.1007/s00208-016-1388-z>.
- [BK19] Hans U. Boden and Homayun Karimi. “The Jones–Krushkal polynomial and minimal diagrams of surface links”. In: *Annales de l’Institut Fourier* 72 (2019), pp. 1437–1475. DOI: [10.5802/aif.3516](https://doi.org/10.5802/aif.3516). URL: <https://doi.org/10.5802/aif.3516>.
- [BK23a] Hans U. Boden and Homayun Karimi. “A characterization of alternating links in thickened surfaces”. In: *Proceedings of the Royal Society of Edinburgh Section A: Mathematics* 153.1 (2023), pp. 177–195. DOI: [10.1017/prm.2021.78](https://doi.org/10.1017/prm.2021.78).
- [BK23b] Hans U. Boden and Homayun Karimi. *Mock Seifert matrices and unoriented algebraic concordance*. 2023. arXiv: [2301.05946v2](https://arxiv.org/abs/2301.05946v2) [math.GT].
- [BLN97] Roland Bacher, Pierre de La Harpe, and Tatiana Nagnibeda. “The lattice of integral flows and the lattice of integral cuts on a finite graph”. eng. In: *Bulletin de la Société Mathématique de France* 125.2 (1997), pp. 167–198. URL: <http://eudml.org/doc/87761>.

- [Bod+15] Hans Boden et al. “Virtual knot groups and almost classical knots”. In: *Fundamenta Mathematicae* 238 (July 2015). DOI: [10.4064/fm80-9-2016](https://doi.org/10.4064/fm80-9-2016).
- [BZH13] Gerhard Burde, Heiner Zieschang, and Michael Heusener. *Knots*. Berlin, Boston: De Gruyter, 2013. ISBN: 9783110270785. DOI: [doi:10.1515/9783110270785](https://doi.org/10.1515/9783110270785). URL: <https://doi.org/10.1515/9783110270785>.
- [CKS00] J. Carter, Seiichi Kamada, and Masahico Saito. “Stable Equivalence of Knots on Surfaces and Virtual Knot Cobordisms”. In: *Journal of Knot Theory and its Ramifications* 11 (Sept. 2000), pp. 311–322. DOI: [10.1142/S0218216502001639](https://doi.org/10.1142/S0218216502001639).
- [CV10] Lucia Caporaso and Filippo Viviani. “Torelli theorem for graphs and tropical curves”. In: *Duke Mathematical Journal* 153.1 (2010), pp. 129–171. DOI: [10.1215/00127094-2010-022](https://doi.org/10.1215/00127094-2010-022). URL: <https://doi.org/10.1215/00127094-2010-022>.
- [GL78] C. Mc Gordon and R. A. Litherland. “On the signature of a link”. In: *Inventiones mathematicae* 47.1 (Feb. 1978), pp. 53–69. ISSN: 1432-1297. DOI: [10.1007/BF01609479](https://doi.org/10.1007/BF01609479). URL: <https://doi.org/10.1007/BF01609479>.
- [Goe34] Lebrecht Goeritz. “Bemerkungen zur knotentheorie”. In: *Abhandlungen aus dem Mathematischen Seminar der Universität Hamburg* 10.1 (June 1934), pp. 201–210. ISSN: 1865-8784. DOI: [10.1007/BF02940674](https://doi.org/10.1007/BF02940674). URL: <https://doi.org/10.1007/BF02940674>.
- [GPV00] Mikhael Goussarov, Michael Polyak, and Oleg Viro. “Finite-type invariants of classical and virtual knots”. In: *Topology* 39.5 (2000), pp. 1045–1068. ISSN: 0040-9383. DOI: [10.1016/S0040-9383\(99\)00054-3](http://dx.doi.org/10.1016/S0040-9383(99)00054-3). URL: [http://dx.doi.org/10.1016/S0040-9383\(99\)00054-3](http://dx.doi.org/10.1016/S0040-9383(99)00054-3).
- [Gre04] Jeremy Green. “A Table of Virtual Knots”. The table up to 4 crossings is available at the listed URL. 2004. URL: <https://www.math.toronto.edu/drorbn/Students/GreenJ/>.
- [Gre11] Joshua Greene. “Lattices, graphs, and Conway mutation”. In: *Inventiones Mathematicae* 192 (Mar. 2011), pp. 717–750. DOI: [10.1007/s00222-012-0421-4](https://doi.org/10.1007/s00222-012-0421-4).
- [Gre17] Joshua Evan Greene. “Alternating links and definite surfaces”. In: *Duke Mathematical Journal* 166.11 (2017), pp. 2133–2151. DOI: [10.1215/00127094-2017-0004](https://doi.org/10.1215/00127094-2017-0004). URL: <https://doi.org/10.1215/00127094-2017-0004>.
- [Gre21] Joshua Greene. “Heegaard Floer Homology”. In: *Notices of the American Mathematical Society* 68.1 (2021), pp. 19–33. DOI: <https://doi.org/10.1090/noti2194>. URL: <https://www.ams.org/notices/202101/rnoti-p19.pdf>.
- [Hat00] Allen Hatcher. *Algebraic Topology*. Cambridge: Cambridge University Press, 2000. URL: <https://pi.math.cornell.edu/~hatcher/AT/AT.pdf>.
- [How17] Joshua Howie. “A characterisation of alternating knot exteriors”. In: *Geometry & Topology* 21.4 (2017), pp. 2353–2371. DOI: [10.2140/gt.2017.21.2353](https://doi.org/10.2140/gt.2017.21.2353). URL: <https://doi.org/10.2140/gt.2017.21.2353>.
- [HP17] Joshua Howie and Jessica Purcell. “Geometry of alternating links on surfaces”. In: *Transactions of the American Mathematical Society* 373 (Dec. 2017). DOI: [10.1090/tran/7929](https://doi.org/10.1090/tran/7929).

- [HTW98] Jim Hoste, Morwen Thistlethwaite, and Jeff Weeks. “The first 1,701,936 knots”. In: *The Mathematical Intelligencer* 20.4 (Sept. 1998), pp. 33–48. ISSN: 0343-6993. DOI: [10.1007/BF03025227](https://doi.org/10.1007/BF03025227). URL: <https://doi.org/10.1007/BF03025227>.
- [Kam02] Naoko Kamada. “On the Jones polynomials of checkerboard colorable virtual links”. In: *Osaka Journal of Mathematics* 39.2 (2002), pp. 325–333.
- [Kar18] Homayun Karimi. “Alternating Virtual Knots”. PhD thesis. McMaster University School of Graduate Studies, Sept. 2018. URL: <https://macsphere.mcmaster.ca/bitstream/11375/23724/2/Homayun%20Karimi%20PhD%20Thesis.pdf>.
- [Kau87] Louis H Kauffman. “State models and the jones polynomial”. In: *Topology* 26.3 (1987), pp. 395–407. ISSN: 0040-9383. DOI: [https://doi.org/10.1016/0040-9383\(87\)90009-7](https://doi.org/10.1016/0040-9383(87)90009-7). URL: <https://www.sciencedirect.com/science/article/pii/0040938387900097>.
- [Kau99] Louis H. Kauffman. “Virtual Knot Theory”. In: *European Journal of Combinatorics* 20.7 (1999), pp. 663–691. ISSN: 0195-6698. DOI: <https://doi.org/10.1006/eujc.1999.0314>. URL: <https://www.sciencedirect.com/science/article/pii/S0195669899903141>.
- [Kin22] Thomas Kindred. *The virtual flying theorem*. 2022. arXiv: [2210.03720](https://arxiv.org/abs/2210.03720) [math.GT].
- [KM06] L. H. Kauffman and V. O. Manturov. “Virtual knots and links”. In: *Proceedings of the Steklov Institute of Mathematics* 252.1 (Jan. 2006), pp. 104–121. ISSN: 1531-8605. DOI: [10.1134/S0081543806010111](https://doi.org/10.1134/S0081543806010111). URL: <https://doi.org/10.1134/S0081543806010111>.
- [Kup03] Greg Kuperberg. “What is a virtual link?” In: *Algebraic & Geometric Topology* 3.1 (2003), pp. 587–591. DOI: [10.2140/agt.2003.3.587](https://doi.org/10.2140/agt.2003.3.587). URL: <https://doi.org/10.2140/agt.2003.3.587>.
- [Lic97] W. B. Raymond Lickorish. *An Introduction to Knot Theory*. Springer New York, NY, 1997. ISBN: 9781461206910. DOI: [doi:10.1007/978-1-4612-0691-0](https://doi.org/10.1007/978-1-4612-0691-0). URL: <https://doi.org/10.1007/978-1-4612-0691-0>.
- [Man13] Vassily Olegovich Manturov. “Parity and Projection from Virtual Knots to Classical Knots”. In: *Journal of Knot Theory and Its Ramifications* 22.09 (2013). DOI: [10.1142/S0218216513500442](https://doi.org/10.1142/S0218216513500442). eprint: <https://doi.org/10.1142/S0218216513500442>. URL: <https://doi.org/10.1142/S0218216513500442>.
- [Mat12] Sergei V Matveev. “Roots and decompositions of three-dimensional topological objects”. In: *Russian Mathematical Surveys* 67.3 (June 2012), p. 459. DOI: [10.1070/RM2012v067n03ABEH004794](https://doi.org/10.1070/RM2012v067n03ABEH004794). URL: <https://dx.doi.org/10.1070/RM2012v067n03ABEH004794>.
- [Men84] W. Menasco. “Closed incompressible surfaces in alternating knot and link complements”. In: *Topology* 23.1 (1984), pp. 37–44. ISSN: 0040-9383. DOI: [https://doi.org/10.1016/0040-9383\(84\)90023-5](https://doi.org/10.1016/0040-9383(84)90023-5). URL: <https://www.sciencedirect.com/science/article/pii/0040938384900235>.

- [MT01] Bojan Mohar and Carsten Thomassen. *Graphs on surfaces*. Johns Hopkins Studies in the Mathematical Sciences. Johns Hopkins University Press, Baltimore, MD, 2001, pp. xii+291. ISBN: 0-8018-6689-8.
- [MT93] William Menasco and Morwen Thistlethwaite. “The Classification of Alternating Links”. In: *Annals of Mathematics* 138.1 (1993), pp. 113–171. ISSN: 0003486X. URL: <http://www.jstor.org/stable/2946636> (visited on 03/27/2023).
- [Mur87] Kunio Murasugi. “Jones polynomials and classical conjectures in knot theory”. In: *Topology* 26.2 (1987), pp. 187–194. ISSN: 0040-9383. DOI: [https://doi.org/10.1016/0040-9383\(87\)90058-9](https://doi.org/10.1016/0040-9383(87)90058-9). URL: <https://www.sciencedirect.com/science/article/pii/0040938387900589>.
- [OS03] Peter Ozsváth and Zoltán Szabó. “Heegaard Floer homology and alternating knots”. In: *Geom. Topol.* 7 (2003), pp. 225–254. ISSN: 1465-3060. DOI: [10.2140/gt.2003.7.225](https://doi.org/10.2140/gt.2003.7.225). URL: <https://doi.org/10.2140/gt.2003.7.225>.
- [OS04] Peter Ozsváth and Zoltán Szabó. “Holomorphic disks and knot invariants”. In: *Adv. Math.* 186.1 (2004), pp. 58–116. ISSN: 0001-8708. DOI: [10.1016/j.aim.2003.05.001](https://doi.org/10.1016/j.aim.2003.05.001). URL: <https://doi.org/10.1016/j.aim.2003.05.001>.
- [OS05] Peter Ozsváth and Zoltán Szabó. “On the Heegaard Floer homology of branched double-covers”. In: *Advances in Mathematics* 194.1 (2005), pp. 1–33. ISSN: 0001-8708. DOI: <https://doi.org/10.1016/j.aim.2004.05.008>. URL: <https://www.sciencedirect.com/science/article/pii/S0001870804001690>.
- [Rei27] Kurt Reidemeister. “Elementare Begründung der Knotentheorie”. In: *Abhandlungen aus dem Mathematischen Seminar der Universität Hamburg* 5 (1927), pp. 24–32. ISSN: 18658784. URL: <https://doi.org/10.1007/BF02952507>.
- [SK19] Kiyoshi Shirayanagi and Yuji Kobayashi. “A new invariant under congruence of nonsingular matrices”. In: *arXiv: Rings and Algebras* (2019).
- [SW10] Yi Su and David G. Wagner. “The lattice of integer flows of a regular matroid”. In: *Journal of Combinatorial Theory, Series B* 100.6 (2010), pp. 691–703. ISSN: 0095-8956. DOI: <https://doi.org/10.1016/j.jctb.2010.07.003>. URL: <https://www.sciencedirect.com/science/article/pii/S0095895610000742>.
- [Thi87] Morwen B. Thistlethwaite. “A spanning tree expansion of the jones polynomial”. In: *Topology* 26.3 (1987), pp. 297–309. ISSN: 0040-9383. DOI: [https://doi.org/10.1016/0040-9383\(87\)90003-6](https://doi.org/10.1016/0040-9383(87)90003-6). URL: <https://www.sciencedirect.com/science/article/pii/0040938387900036>.
- [Whi33] Hassler Whitney. “2-Isomorphic Graphs”. In: *American Journal of Mathematics* 55.1 (1933), pp. 245–254. ISSN: 00029327, 10806377. URL: <http://www.jstor.org/stable/2371127> (visited on 03/21/2023).

Appendix A Python Implementation of Algorithms

A Python implementation of the algorithms given in this essay, along with the results of the computations is available at:

<https://github.com/DamianJLin/msmat>

In particular:

- The tabulation of alternating virtual knots up to 6 crossings based on a list provided by Hans Boden and created by Lindsay White from Jeremy Green's tabulation [Gre04] can be found in the file `data/alternating_virtual_6.txt`
- The results of the Gordon-Litherland pairing matrix computations can be found in the file `data/gordonlitherland_6_bygenus.txt`
- The results of the mock Seifert matrix computations can be found in the file `data/mockseifert_6_bygenus`

Matrix computations of virtual knots are sorted by virtual genus.